Time scales and mechanisms of uranium uptake in altered ocean crust; observations from the ~15 million year-old site 1256 in the eastern equatorial Pacific

Morten B. Andersen [a,*], Joel B. Rodney [b], Heye Freymuth [c], Flurin Vils [b,d], Michelle Harris [e], Kari Cooper [f], Damon A.H. Teagle [g], Tim Elliott [b]

[a] School of Earth & Environmental Sciences, Cardiff University, Park Place, CF10 3AT Cardiff, United Kingdom
[b] School of Earth & Environmental Sciences, University of Bristol, Wills Memorial Building, Queen Street, BS8 1RJ Bristol, United Kingdom
[c] Department of Earth Sciences, University of Cambridge, Downing Street Cambridge, Cambridgeshire CB2 3EQ, United Kingdom
[d] Wanner Geologie und Umweltfragen, Dornacherstrasse 29, 4500 Solothurn, Switzerland
[e] School of Geography, Earth & Environmental Sciences, University of Plymouth, B526 Portland Square, Drake Circus, Plymouth PL4 8AA, United Kingdom
[f] Department of Earth and Planetary Sciences, University of California Davis, One Shields Ave., Davis, CA 95616, USA
[g] School of Ocean & Earth Science, National Oceanography Centre Southampton, University of Southampton, SO14-3ZH Southampton, United Kingdom

ARTICLE INFO

ABSTRACT

The alteration of ocean crust through hydrothermal seawater circulation facilitates chemical exchange between Earth's surface and interior. Hydrothermal alteration leads to uranium (U) removal from seawater and net U uptake by the ocean crust, particularly during low temperature alteration that occurs on the vast ocean ridge flanks away from the spreading axes. Determining the timescales of U uptake and its associated $^{238}U/^{235}U$ signature has important implications for understanding U exchange processes during subduction and recycling into the mantle. Here we study the U systematics of ~15 million year-old ocean crust drilled at Site 1256 on the eastern flank of the East Pacific Rise. Analysis of cores from the upper ~1300 m of intact ocean crust at this site, reveal large variability in U concentrations and $^{238}U/^{235}U$ ratios. Many of the samples from the upper ~600 m of extrusive lavas have elevated U concentrations and $^{238}U/^{235}U$ ratios lower than seawater, consistent with mechanisms of U uptake under relatively oxidised conditions. Samples from the underlying sheeted dikes and gabbros show evidence for hydrothermal U mobilisation, but negligible net U uptake. In contrast, in the transition zone between the extrusive lavas and the sheeted dikes, samples revealed large U enrichments and high $^{238}U/^{235}U$ ratios above seawater. This is consistent with uptake of the reduced U^{+4} species under relatively reducing conditions from seawater-derived hydrothermal fluids. In addition, large secular disequilibrium in $^{234}U/^{238}U$ ratios from samples in the lava-dike transition and upper sheeted dikes give evidence for U mobility within the last ~1.5 million years, likely driven by deep channelled flow of seawater-derived hydrothermal fluids combined with preferential leaching of ^{234}U from the rock matrix. Both the total estimated U uptake and mean $^{238}U/^{235}U$ at Site 1256 is lower than similar estimates from significantly older (>100 million years) altered ocean crusts at drill Sites 801 and 417/418. This shows the variable total U uptake and $^{238}U/^{235}U$ ratio in altered ocean crust over time, which needs to be taken into consideration when estimating global U budgets.

1. Introduction

The formation of new ocean crust at mid-ocean ridge axes and its recycling into the mantle by subduction enables chemical exchanges between Earth's surface and mantle reservoirs. These exchanges occur via high temperature (up to ~400 °C) circulation of seawater-derived fluids at the spreading ridges driven by heat from the cooling and crystallisation of new ocean crust, and lower temperature (<100 °C)

* Corresponding author

E-mail addresses: andersenm1@cardiff.ac.uk (M.B. Andersen), joel.rodney@bristol.ac.uk (J.B. Rodney), hf325@cam.ac.uk (H. Freymuth), fv@wanner-so.ch (F. Vils), michelle.harris@plymouth.ac.uk (M. Harris), kmcooper@ucdavies.edu (K. Cooper), damon.teagle@southampton.ac.uk (D.A.H. Teagle), tim.elliott@bristol.ac.uk (T. Elliott).

exchanges on the ocean ridge flanks (e.g. Alt, 1995; Elderfield and Schultz, 1996; Staudigel, 2014). These processes lead to seawater-driven weathering and alteration of the ocean crust, inducing chemical exchanges with potential losses and gains of elements (e.g., magnesium, potassium, rubidium, uranium, carbon; Albarède and Michard, 1986; Alt and Teagle, 1999; Dunk et al., 2002; Staudigel, 2014). Characterisation of the alteration signatures in the ocean crust is important for establishing the heat exchange between mantle and the ocean (e.g. Elderfield and Schultz, 1996; Staudigel, 2014; Stein and Stein, 1994), geochemical budgets of elements in the ocean (e.g. Albarède and Michard, 1986; Staudigel, 2014) and the fluxes of surface-derived components into arc systems and the residual proportion transported further into the mantle (e.g. Plank and Manning, 2019). These alteration processes can be gauged from changes in geochemical signatures, either
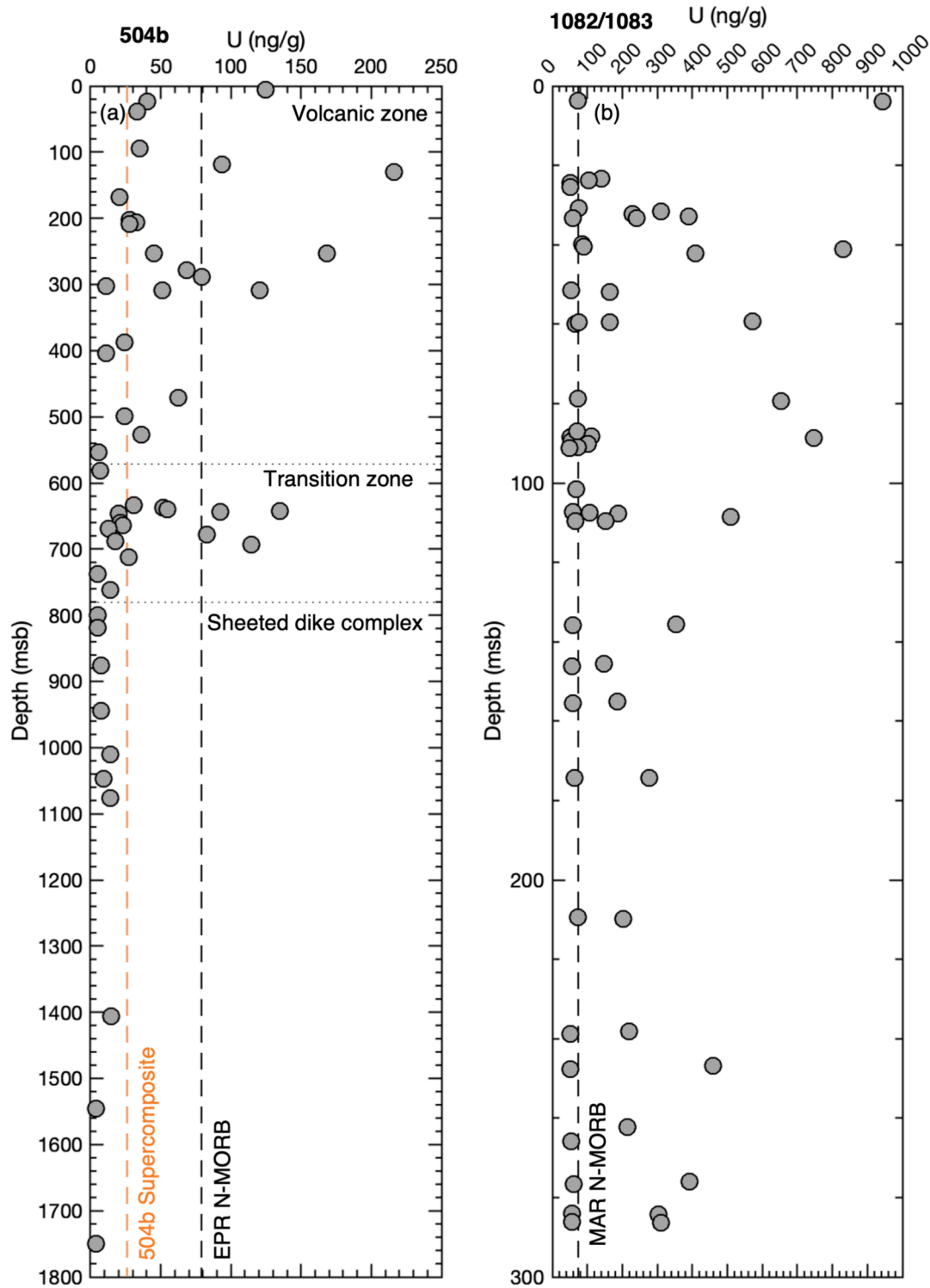
Fig. 1. Published U concentrations with depth below sub-basement for (a) Site 504B (Pacific ~5.9 Ma: Bach et al., 2003), and Site 1082/1083 (Atlantic, ~8 Ma; Türke et al., 2015). In (a) reference lines for average East Pacific rise (EPR) N-MORB and estimated unaltered MORB at 504B (Bach et al., 2003) is plotted, while lithological depth sections are separated into lava, transition and sheeted dike. In (b) reference line for average mid-Atlantic ridge (MAR) N-MORB is plotted.

based on diagnostics in major and trace metal compositions or isotope systematics (e.g. Staudigel, 2014). For example, the seawater and ocean crust exchange of strontium (Sr) during alteration has a major impact on the $^{87}Sr/^{86}Sr$ signature of seawater (e.g. Palmer and Edmond, 1989; Vance et al., 2009) and the distinctive $^{238}U/^{235}U$ ratios of the uranium (U) uptake in altered ocean crust has been used to identify the recycling of surfaced-processed U into the mantle (Andersen et al., 2015). However, usage of such geochemical tools requires the rigorous characterisation of the variations in composition of altered ocean crust. Although relatively homogeneous compared to the continents, ocean crust still shows significant variations in alteration style with spreading rate and age as it cools, subsides and becomes covered by sediments with maturation away from the ocean ridges (e.g. Staudigel, 2014).

Uranium is a sensitive tracer of surface exchange processes because it has relatively high concentrations in seawater (~3.3 ng/g), its solubility is sensitive to oxidation conditions and it presents isotopic ratios useful for fingerprinting sources and timings of processes (e.g. Andersen et al., 2015; Bacon, 1978). Uranium is, on average, taken up by the ocean crust during exchanges with seawater-derived hydrothermal fluids (e.g. Dunk et al., 2002; Kelley et al., 2005; Staudigel et al., 1995). The impact of the most intense, near-axis high-temperature hydrothermal alteration is not well quantified, but discharging black smoker-type fluids have low U concentrations, suggesting near-quantitative U removal within the ocean crust (Chen et al., 1986; Michard et al., 1983; Mottl et al., 1998). Given the much larger potential for low-temperature seawater-basalt exchange during hydrothermal alteration on the ocean ridge flanks, it is likely that this dominates U uptake within the ocean crust (e.g. Alt et al., 2010; Bach et al., 2003; Dunk et al., 2002; Kelley et al., 2005; Staudigel et al., 1995). The low-temperature U addition initially occurs under relatively oxidised conditions at high water-to-rock ratios, leading to U^{+6} uptake associated with secondary alteration phases such as iron-oxyhydroxides and celadonite (e.g. Bach et al., 2003; Mitchell and Aumento, 1977; Türke et al., 2015). However, the formation of secondary minerals and the accumulation of sediments as the crust ages away from the ridge axis can impede the direct recharge of oxygenated seawater into the ocean crust leading to lower water-to-rock ratios and more reducing conditions with U^{+4} uptake associated with the formation of, for instance, secondary Mg-saponite, pyrite and carbonates (e.g. Alt and Teagle, 2003; Dunk et al., 2002; Kelley et al., 2005; Staudigel, 2003). The intensity of different alteration processes is linked to the specific lava morphology and thermal evolution of individual ocean crustal sections, leading to heterogeneous addition of U to the ocean crust (e.g. Alt and Teagle, 2003; Dunk et al., 2002; Kelley et al., 2003). Estimates to date based on drilled sections of altered upper ocean crust from a range of crustal ages (3–167 million years), indicate on average a 5- to 10-fold increase in U concentration in the upper ~1000 m (Fig. 1), compared to unaltered ocean crust (Dunk et al., 2002; Kelley et al., 2005; Staudigel, 2003).

In addition, U isotope systematics offer further insight into U uptake mechanisms and time scales of seawater-basalt exchanges. The ~245 thousand year half-life of the ^{234}U daughter compared to its much longer lived parent ^{238}U (Cheng et al., 2013), means that the preservation of secular disequilibrium in the $^{234}U/^{238}U$ ratio implies perturbation within the last ~1.5 million years. Here, $^{234}U/^{238}U$ ratios are expressed as $\delta^{234}U$, where the $^{234}U/^{238}U$ ratio of the sample is normalized to secular equilibrium and reported in parts per thousand, such that at secular equilibrium $\delta^{234}U = 0$. Low-temperature weathering processes have been shown to cause significant disequilibrium in the $^{234}U/^{238}U$ ratio due to alpha-recoil induced preferential redistribution of the ^{234}U daughter nuclide, generally leading to ^{234}U excesses in fluids and depletions in leached solid residues (e.g. Andersen et al., 2009; Kigoshi, 1971; Porcelli and Swarzenski, 2003). For instance, modern seawater is characterized by a $\delta^{234}U$ of ~+145 ‰ (Kipp et al., 2022) principally due to the input of high $\delta^{234}U$-bearing waters from rivers (e.g. Dunk et al., 2002). Consequently, $^{234}U/^{238}U$ ratios have the potential to provide chronological constraints on the processes of U addition from seawater

and hydrothermal fluid leaching processes (e.g. Bacon, 1978; Macdougall et al., 1979).

Furthermore, a rapidly growing data-base of $^{238}U/^{235}U$ ratios from different Earth reservoirs has revealed large natural variability (e.g. Andersen et al., 2017 and references therein). In the following $^{238}U/^{235}U$ ratios are expressed using the $\delta^{238}U$ notation which is the relative difference of the $^{238}U/^{235}U$ ratio of a sample compared to the standard CRM 145, expressed in parts per thousand. The main driver of $^{238}U/^{235}U$ fractionations are differences in bonding environment between U species in its two common redox states +4 and +6 (Bigeleisen, 1996). Uranium uptake or exchange with no redox change, under oxidised conditions (e.g., +6 species) generally leads to slightly lower $\delta^{238}U$ values in the solid product – for example, the <0.2 ‰ lowering of $^{238}U/^{235}U$ ratios by U uptake from seawater to ferro-manganese-oxides (e.g. Brennecka et al., 2011; Goto et al., 2014). In contrast, under more reducing conditions, the isotope fractionation between soluble U^{+6} and immobile U^{+4} may inflict large, per mil level, changes with higher $\delta^{238}U$ in the reduced product (e.g. Bigeleisen, 1996; Stirling et al., 2007; Weyer et al., 2008). Measured $\delta^{238}U$ values in ~120 to ~170 million year-old ocean crusts from drill Sites 417/418 in the Atlantic and 801 in the Pacific (Fig. 2) illustrate this, showing both isotopically lighter and heavier signatures compared to the compositions of the near-homogenous open-ocean seawater (−0.38 ± 0.02; Kipp et al., 2022), the average continental crust (−0.30 ± 0.03; Tissot and Dauphas, 2015) and average mid-ocean ridge basalts (−0.26 ± 0.03; Andersen et al., 2015). The processes of U uptake in altered ocean crust have been shown to lead to significant $\delta^{238}U$ variability, measured in bulk samples (−0.47 to +0.27 ‰), calcium carbonate phases (−0.63 to +0.11 ‰) and 'composite' samples (−0.49 to +0.23 ‰), the latter representing average sections of altered ocean crust (Andersen et al., 2015; Noordmann et al., 2016; see also review in Andersen et al., 2017). Such variations in $\delta^{238}U$ values indicate that heterogenous and non-quantitative addition of seawater-derived U occurs during the alteration of the ocean crust (Fig. 2).

This previous work (Andersen et al., 2015; Noordmann et al., 2016) provides some indication of the overall systematics of $\delta^{238}U$ within old (>100 Ma) altered ocean crust. However, there is a current lack of information on the temporal evolution of the U isotope systematics as ocean crust ages away from the ridge axis. Additional temporal constraints are important to accurately quantify U exchange and isotopic composition estimates for the marine budget and for subducting ocean crust. Although conductive heat flow deficits are present in all ocean basins out to ~65 million years (e.g. Elderfield and Schultz, 1996; Staudigel, 2014; Stein and Stein, 1994), $\delta^{234}U$ values can provide additional geochemical evidence for the timing and duration of low-temperature hydrothermal alteration of the ocean crust. Here we perform a comprehensive study of U uptake and isotope systematics ($^{234}U/^{238}U$ and $^{235}U/^{238}U$ ratios) at depth, for a complete section of intact upper ocean crust from lavas, through the sheeted dikes and into the uppermost gabbros from Ocean Drilling Program (ODP) Site 1256, drilled into crust formed 15 million-years ago at the fast spreading East Pacific Rise (Wilson et al., 2006).

2. Site 1256 and sample descriptions

Holes 1256C and 1256D (Fig. 3) were drilled in the eastern equatorial Pacific (6.736°N, 91.934°W) during four scientific ocean drilling cruises (ODP Leg 206; IODP Expeditions 309/312, 335; Teagle et al., 2012; Wilson et al., 2006). Site 1256 is in a region of relatively smooth seafloor topography (<10 m relief) although there is a trail of ~500 m-high seamounts 15–20 km north-east. Sediment porewater and heat flow measurements at Site 1256 indicate that there is no current evidence for fluid circulation or advective heat transport at the seafloor (Alt et al., 2010; Teagle et al., 2012). From the seafloor, Holes 1256C/D penetrate ~250 m of sediments, (1) ~750 m of extrusive lavas, (2) a ~60 m-thick lava-dike transition zone, mineralised in places, (3) ~350 m of sheeted
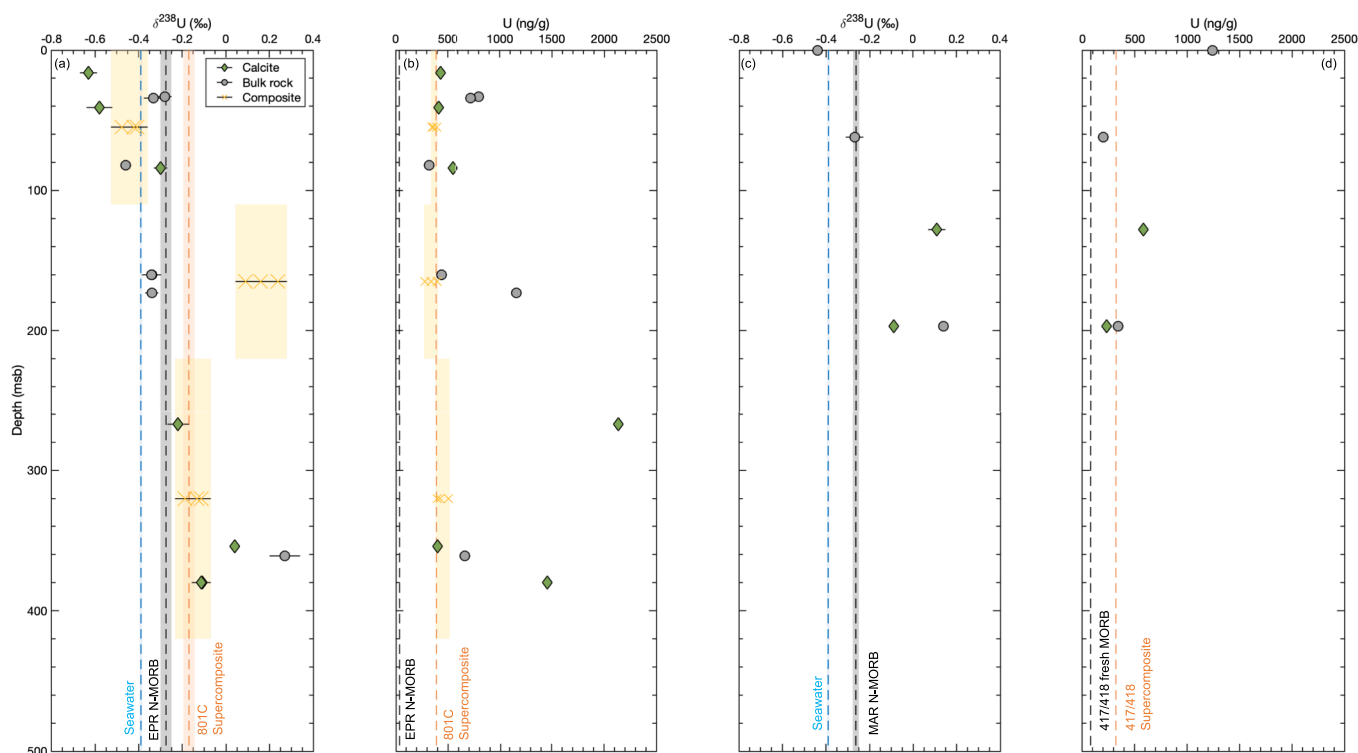
Fig. 2. Published $\delta^{238}U$ compositions (a,c) and U concentrations (b,d) vs. depth below sub-basement from (a,b) Pacific Site 801B/C and (c,d) Atlantic Site 417/418, respectively. The top of both cores is at the sediment to ocean crust transition. Discrete samples and composite samples are shown (see legend). In Site 801, 'composite samples' (mixtures of the different lithologies and alteration styles, blended as powders in representative proportions (Plank et al., 2000) from 0–110 m, 110–220 m and 220–420 m are shown as horizontal lines and shaded area covers the depth range. Composites are marked with the stippled yellow line, with the band around the line representing the variability of the composites within the section ($\delta^{238}U$ for 801 and U conc. for 801 and 417/418). Reference lines are shown for seawater and Pacific/Atlantic N-MORB for the $\delta^{238}U$ composition, and average Pacific or Atlantic MORB for U concentration. Data sources: discrete samples are from Noordmann et al. (2016) and Andersen et al. (2015); $\delta^{238}U$ for composites, seawater and Pacific/Atlantic MORB from Andersen et al. (2015) and Kipp et al. (2022); Pacific N-MORB U concentration from Andersen et al. (2015); Atlantic MORB and composite U concentration from Staudigel et al. (1989); 801 composite U concentration Kelley et al. (2003).

dikes and (4) ~120 m into a dike-gabbro transition zone (Teagle et al., 2012). A thorough description of rock types and estimates of hydrothermal alteration temperatures (from major and trace elements, mineralogy, O isotopes and fluid inclusions in alteration products) can be found in Alt et al. (2010). Subsequent analyses of samples from Site 1256 include Sr, Nd, Pb, Li, Mg and O isotope ratios (Gao et al., 2012; Harris et al., 2015; Höfig et al., 2014; Huang et al., 2015) and trace metal abundances (Höfig et al., 2014; Patten et al., 2016). Furthermore, U concentration and Th/U ratio systematics of 36 samples were investigated in Höfig et al. (2014) whereas a comprehensive Th/U ratio dataset of 462 samples are available from the Ph.D. thesis of Harris (2011). In this study, 49 representative samples were selected for U isotope analyses to provide coverage of the four main units and alteration styles at Site 1256. The majority of the samples chosen (41 out of the 49) have been analysed previously for other tracers, including radiogenic Sr isotope ratios (Harris et al., 2015). The analysed samples are described below, grouped into four main sections of the altered ocean crust, including details on lithology and alteration style.

2.1. Extrusive lava section (0–754 m sub-basement; msb)

A total of 23 samples (21 and two from the deep Hole 1256D and C, respectively) were selected to cover the upper extrusive lava section. The upper ~284 msb of lavas are interpreted to have flowed from the ridge axis, whereas the lower part of the lava sequence have been formed at the ridge axis (see Harris et al., 2015; Teagle et al., 2006). The uppermost ocean crust comprises a sequence of lavas dominated by a single ponded lava flow up to 75 m thick. Below this the extrusive rocks

comprise of sheet and massive flows with only minor pillow lavas (Alt et al., 2010; Teagle et al., 2012; Tominaga et al., 2009; Wilson et al., 2006). Low-temperature alteration (<150 °C) from seawater-derived fluids dominates in the extrusive lava section, with later stages of alteration following existing fluid pathways (Alt et al., 2010; Gao et al., 2012). A range of alteration styles is present with a background of moderate alteration to dark grey colour and dark grey patches (mm to cm size) of saponite replacement with secondary sulfides and variable amounts of chlorite (Alt et al., 2010; Teagle et al., 2012). Veins and associated alteration halos up to 3 cm wide, dominated by a brownish (including celadonite and iron-oxyhydroxide phases) and darker colours (saponite), are interpreted to have derived from oxidised, hydrothermally heated seawater. Carbonates make up a few percent of the material and some anhydrite is present in the lowest part of the extrusive lava section. A general change in alteration style occurs below ~377 msb with more intense saponite and chlorite alteration. At 398 msb there is a ~40 cm band of intense bulk rock alteration to celadonite, K-feldspar and iron oxyhydroxide (±quartz and carbonate), known as the 'red brick horizon' (Alt et al., 2010; Harris et al., 2015). The ~750 m extrusive lava sequence is generally less hydrothermally altered than other deep mafic ocean crust sites (e.g. Sites 417/418, and Hole 504B; Alt, 1995) and Site 1256 does not show a general systematic change from oxidizing to reducing alteration style with depth, as seen in Hole 504B (Alt et al., 2010). Instead, oxidizing alteration occurs irregularly, commonly near vertically dipping veins, suggesting a structural control of alteration, rather than simply decreasing seawater influence downwards (Wilson et al., 2006). The early effective sealing of the basement from ocean waters due to high rates of sedimentation at this site (>30
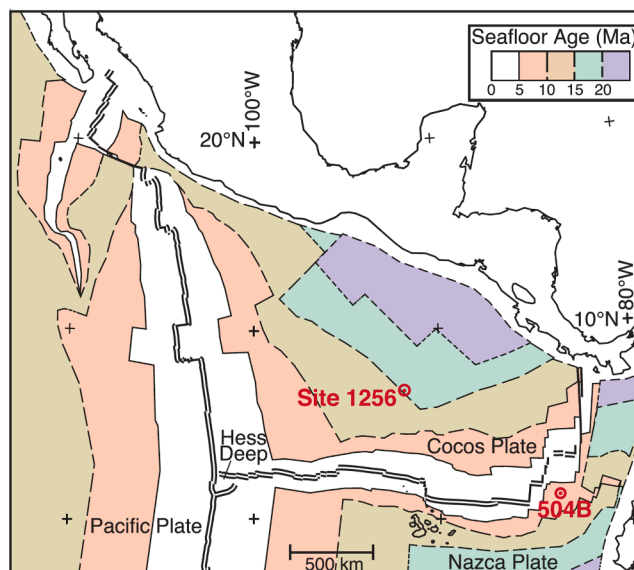
Fig. 3. Map showing the locations of Sites 1256 and 504 in the eastern equatorial Pacific with crustal ages shown in 5 million year intervals (modified from Wilson et al., 2003).

m/million years; Wilson et al., 2003) and the massive ponded lava that makes up the uppermost crust at Site 1256 could have limited the ingress of seawater, thereby leading to the overall lower level of alteration compared to other sites (Alt et al., 2010; Gao et al., 2012; Harris et al., 2015; Höfig et al., 2014). Samples analysed are distributed across the section to cover the different lava (pond, pillows, sheeted and massive flows) and alteration (background, haloes, patchy, 'red brick') styles. Although most were analysed as whole rock samples, samples 26R-2 70–80 and 62R-1 16–21 at ~190 and 437 msb, respectively, were separated into predominantly 'fresh' and 'halo' parts (Supplementary Table 1).

2.2. Lava-dike transition zone (754–811 msb)

The lithological transition zone is marked by subvertical intrusive contacts and mineralized hyaloclastic breccias. There is a step-wise increase in alteration temperature from the extrusive lavas above and into the sections below (to > 250 °C), with the transition zone characterized by sub- to greenschist mineral alteration. Hydrothermal alteration halos along veins, highly altered patches and localised metal-sulfide mineralization in breccias and veins, occur. Chlorite is a major alteration phase, and some anhydrite is present. The transition zone includes a ~3 m thick mineralized hyaloclastite breccia (777–780 msb), where glass shards are replaced by albite, oligoclase, K-feldspar and titanite, cemented by quartz and pyrite ± sphalerite, anhydrite and calcite (Alt et al., 2010). Radiogenic strontium isotope ratio measurements from this mineralized breccia indicates it is a mixing zone between seawater-derived low-temperature fluids and upwelling high-temperature hydrothermal fluids (Alt et al., 2010; Harris et al., 2015; Höfig et al., 2014). A total of nine samples were analysed from the lithological lava-dike transition zone, with samples collected focussed on the mineralized hyaloclastite breccia, including sample 112R-X 96–100 at 778 msb that was divided into 'breccia' and 'clast' subsamples.

2.3. Sheeted dike complex (811–1157 msb)

The ~350 m thick sheeted dike complex contains doleritic textures and cross-cutting of subvertical dikes with mineralised chilled margins (Wilson et al., 2006). Similar to the lava-dike transition, the upper sheeted dikes are characterized by sub- to greenschist alteration with hydrothermal alteration halos along veins, highly altered patches and

local metal-sulfide mineralization. Anhydrite precipitation occurs in the upper section (dominantly between 850 and 950 msb) and is interpreted to have been formed from partially reacted heated seawater-derived fluids mixing with hotter magmatic-derived hydrothermal fluids from below (Alt et al., 2010). The general pattern of alteration suggests early stages of high temperature greenschist alteration (>350 °C) followed by fracture-controlled alteration with upward migrating hydrothermal fluids and leaching of some metals (e.g. Zn, Cu) from the deeper sheeted dikes and gabbro sections, followed by sulfide-precipitation in the upper sheeted dikes and lava-dike transition (Alt et al., 2010; Patten et al., 2016). The lowermost ~60 m of the sheeted dikes (1098–1157 msb) are strongly recrystallised to granoblastic textures. Twelve samples were selected from the sheeted dike complex, chosen to cover a range of background rocks and alteration patches.

2.4. Plutonic dike-gabbro transition (below 1157 msb)

The crust below 1157 msb comprises a series of gabbro bodies intruded into contact metamorphosed sheeted dikes (Wilson et al., 2006). Early high-temperature alteration (500–1000 °C) is evident in metamorphic assemblages and textures (e.g. metamorphic clinopyroxene and amphibole) and the loss of Cu and Zn to hydrothermal fluids (Alt et al., 2010). Five samples were selected for analyses from this zone covering the gabbroic sections.

3. Methods

The U isotope and concentration measurements generally followed Andersen et al. (2015), and readers are referred to this for thorough information, with a brief description below.

3.1. Sample preparation, U purification and elemental concentrations

All samples were powdered prior to chemical processing (see Harris et al., 2015). Chemical processing and analyses were done in the laboratories of the Bristol Isotope Group, University of Bristol. Sample sizes from 0.1 to 1.5 g were dissolved in a mixture of concentrated HF-HNO$_3$ acid and spiked with the IRMM-3636 ^{233}U-^{236}U double spike (Richter et al., 2008) aiming for ^{236}U/^{235}U ratios of ~5. This sample-spike mixture was heated on a hotplate at 120 °C before being dried down. Samples were then twice redissolved in hot 6 N HCl before being dried

down. Samples were then redissolved in 1.5 N HNO_3. For samples with unknown U and Th concentrations a small (1 %) aliquot of the dissolved sample was taken for elemental concentration determination using an Element 2 ICP-MS (following Andersen et al., 2013). The U was separated from all other matrices in a two-step procedure consisting of first TRU Resin and then UTEVA chromatographic columns (Andersen et al., 2015). After the UTEVA chemistry step, samples were re-dissolved in an appropriate amount of 0.2 N HCl for the desired U concentration for the MC-ICPMS measurements. Near full uranium recoveries (>95 %) were obtained for the samples and total full procedural U chemistry blanks were <20 pg.

3.2. Uranium isotope measurements

The U isotope measurements were conducted on a Thermo Finnigan Neptune MC-ICP-MS (Serial No. 1002), running in low mass resolution (M/ΔM ~ 500), using an Aridus desolvating nebulizer introduction system and a standard and X cones setup (see Andersen et al., 2015). Given the variability in U concentrations of the samples, a range of sample sizes were processed to give enough U for analyses (10–200 ng). To optimise precision and accuracy two different measuring protocols were used depending on the amount of U available; a 'high' and 'low' precision set-up (~1 nA and ~100 pA for the ^{238}U beam intensities, respectively). In the 'low' precision set-up, Faraday cups were connected to amplifiers with 10^{11} Ω feedback resistors (Andersen et al., 2014), and the minor ^{234}U beam was either collected in a 10^{11} Ω feedback resistors Faraday cup or, to improve the precision on $^{234}U/^{238}U$ ratios, in a secondary electron multiplier (following previous setup of this method for ^{234}U collection; Andersen et al., 2013). For the 'high' precision set-up, amplifiers with 10^{11} Ω feedback resistors were used apart from the cup collecting the ^{238}U beam which was connected to an amplifier with a 10^{10} Ω feedback resistor to accommodate a larger ion beam and so facilitate a greater dynamic range (Andersen et al., 2015).

Measurements of all unknown samples were bracketed and normalised to measurements of the CRM-145 standard, spiked with IRMM-3636 in a similar fashion as the unknown samples. Corrections for mass bias, tailing, hydride interferences, impurities of natural U isotopes in the spike, as well as on-peak background subtractions were performed following Andersen et al. (2015). The external reproducibilities of the two different measurement set-ups were tested using the in-house uraninite standard CZ-1. Interspersed measurements of the CZ-1 for the 'high' precision set-up gave a $δ^{238}U$ of −0.03 ± 0.03 ‰ and a $δ^{234}U$ of 0 ± 3 ‰ (all ± 2 standard deviations), whereas a single measurement of the chemically processed BHVO-2 standard yielded a $δ^{238}U$ of −0.32 ± 0.02 ‰ and a $δ^{234}U$ of 0 ± 1 ‰. The CZ-1 measurements for the 'low' precision set-up gave a $δ^{238}U$ of −0.05 ± 0.11 ‰ and a $δ^{234}U$ of +0.2 ± 0.4 ‰ when using the secondary electron multiplier and −2 ± 4 ‰ using the Faraday cup for ^{234}U collection (see Supplementary Table 2 for standard data). These results agree well with previous measurements of CZ-1 and BHVO-2 (Andersen et al., 2015; Li and Tissot, 2023). The associated uncertainties for the Site 1256 samples reported in the following are based on the reproducibility (2SD) for the repeated measurements of CZ-1 in the two different set-ups, scaled to the internal errors (2SE) of the samples. Namely, if internal errors for the unknown were smaller than the average internal errors reported for the CZ-1 standard, the external reproducibility for the CZ-1 was used. If internal errors for the unknowns were larger than the average internal error of the CZ-1, the estimated uncertainties of the unknowns were scaled up proportionally compared to the external standard reproducibility of the CZ-1 standard.

4. Results

The data is grouped into the four principal stratigraphical sections of altered ocean crust at Site 1256 as described in section 2 (see Supplementary Table 1). Each section shows variable U concentrations, Th/U

ratios and uranium isotope systematics (Fig. 4). Comparison of U concentrations vs. Th/U ratios of all the data show a general inverse correlation with higher U concentrations corresponding to lower Th/U ratios (Fig. 5). The data-set of Harris (2011) is the most comprehensive for U concentrations and Th/U ratios (n = 462) and separating these data into the four major stratigraphic sections, it shows a pattern of dominantly higher U concentrations in the extrusive lavas (mean U ~ 117 ng/g) and lava-dike transition zone (mean U ~ 502 ng/g), here elevated from the samples in the breccia zone, compared to the sheeted dikes (mean U ~ 52 ng/g) and plutonic dike-gabbro section (mean U ~ 65 ng/g) (Table 1). The mean Th/U ratios for the stratigraphic sections are lower for the upper extrusive lavas and lava-dike transition zone (both ~2.4 g/g) compared to the sheeted dikes and plutonic dike-gabbro section (~3.3 and ~4.4 g/g, respectively). The mean Th/U ratios for the stratigraphic sections can also be estimated by weighting the samples by their Th and U concentrations. This approach lowers the mean Th/U ratios for all stratigraphic sections based on the Harris (2011) data, most significantly for the lava-dike transition and the plutonic dike-gabbro sections (0.4 and 2.9 g/g, respectively, see Table 1). The overall mean of all the data yields U concentrations of 93 ng/g and mean Th/U ratios of either 3.0 or 2.1 g/g (if Th-U concentration-weighted). Omitting all the data from below the sheeted dikes, only marginally increases the mean U concentration and lowers the mean Th/U ratios (Table 1). Furthermore, if mean U concentrations and Th/U ratios are weighted proportionally to the thickness of each stratigraphic unit (excluding the plutonic dike-gabbro), this also only marginally increases the mean U concentration (~113 ng/g) and lowers the mean Th/U ratios (2.8 or 1.8 g/g for the Th-U concentration-weighted; see Table 1).

At Site 1256, the $δ^{238}U$ show the largest variability in the extrusive lava section, particularly in the upper 300 m, with $δ^{238}U$ ranging from −0.18 ± 0.20 ‰ and down to the lowest value of −1.02 ± 0.03 ‰. The lava-dike transition section also shows large variability, with the highest $δ^{238}U$ of −0.03 ± 0.03 ‰ ranging down to −0.60 ± 0.03 ‰. Both the sheeted dike and plutonic dike-gabbro transition sections show less variable $δ^{238}U$ with values from −0.16 ± 0.06 to −0.42 ± 0.10 ‰ and −0.18 ± 0.10 to −0.53 ± 0.10 ‰, respectively. A plot of U concentrations versus $δ^{238}U$ shows some overall systematic behaviour in the extrusive lavas and lava-dike transition (Fig. 6). The extrusive lava samples with low $δ^{238}U$ generally correspond to samples with elevated U concentrations compared to mean normal mid-ocean ridge basalts (N-MORB). Samples from the lava-dike transition zone show increasing U concentrations with increasing $δ^{238}U$ (up to −0.03 ± 0.02 ‰) for the samples up to ~1000 ng/g. Samples with U concentrations greater than ~1000 ng/g, show an inverse trend with decreasing $δ^{238}U$, reaching −0.41 ± 0.02 ‰, at the highest U concentration (Fig. 6). One sample from lowermost part of the lava-dike transition just above the top of the sheeted dikes does not follow this described trend, but has low $δ^{238}U$ value (−0.60 ± 0.03 ‰) with moderately elevated U concentration (~210 ng/g) (Fig. 6).

The 'fresh' and the 'halo' sample pairs show both variable U concentrations and $δ^{238}U$. At 190 msb, both the 'fresh' and the 'halo' fractions show elevated U concentration (157 and 119 ng/g) compared to the mean Pacific N-MORB. Although the 'halo' sample (−0.26 ± 0.10 ‰) has a $δ^{238}U$ value overlapping with Pacific N-MORB, the 'fresh' sample has a lower $δ^{238}U$ value (−0.63 ± 0.10 ‰). The paired samples at 437 msb have lower U concentrations (71 and 83 ng/g) than the pair at 190 msb and $δ^{238}U$ that overlap within uncertainty. The 'fresh' sample (−0.25 ± 0.10 ‰) is similar to mean Pacific N-MORB whereas the 'halo' is slightly lower (−0.43 ± 0.10 ‰). The paired 'clast' and 'breccia' sample from 778 msb in the lava-dike transition zone both have high U concentrations (278 and 780 ng/g, respectively) combined with relatively high, albeit slightly variable $δ^{238}U$ (−0.12 ± 0.03 and −0.03 ± 0.03 ‰).

The $δ^{234}U$ of the whole data-set show that 34 of 49 samples are out of secular equilibrium when taking into account the associated measurement uncertainties, with three below and 31 above secular equilibrium.
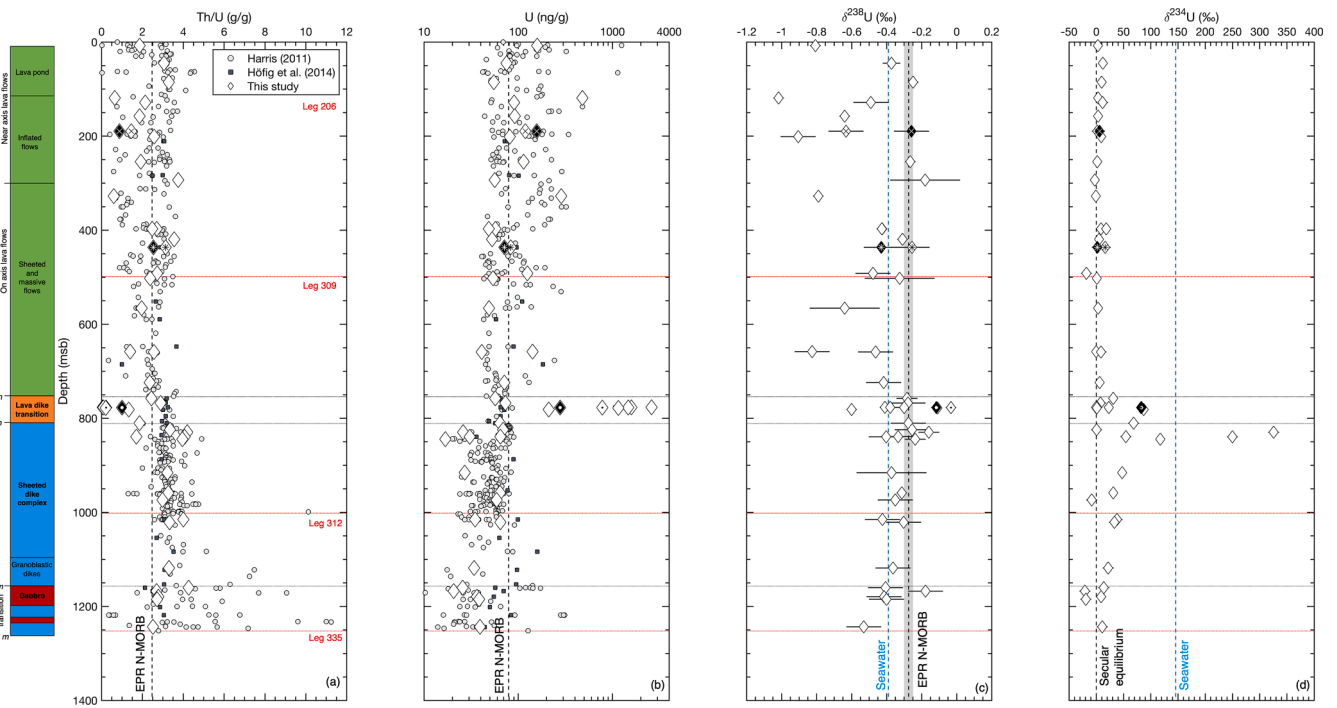
Fig. 4. Stratigraphic depth (msb) section of Site 1256 versus Th/U ratios, U concentrations (logarithmic scale), $\delta^{238}U$ and $\delta^{234}U$ values. Lithologies and stratigraphic sections are labelled on the left, boundaries between stratigraphic sections are marked with grey horizontal lines, while the boundaries between sections recovered in different drilling expeditions are marked with red stippled lines (Teagle et al., 2006; Teagle et al., 2012; Wilson et al., 2006). Average compositions for EPR MORB (in Th/U and U concentrations), seawater (blue dashed in $\delta^{238}U$ and $\delta^{234}U$), 801 composite (dark dashed with grey ± uncertainty $\delta^{238}U$) and secular equilibrium (grey dashed $\delta^{234}U$) are shown as vertical lines (references as in Fig. 1).
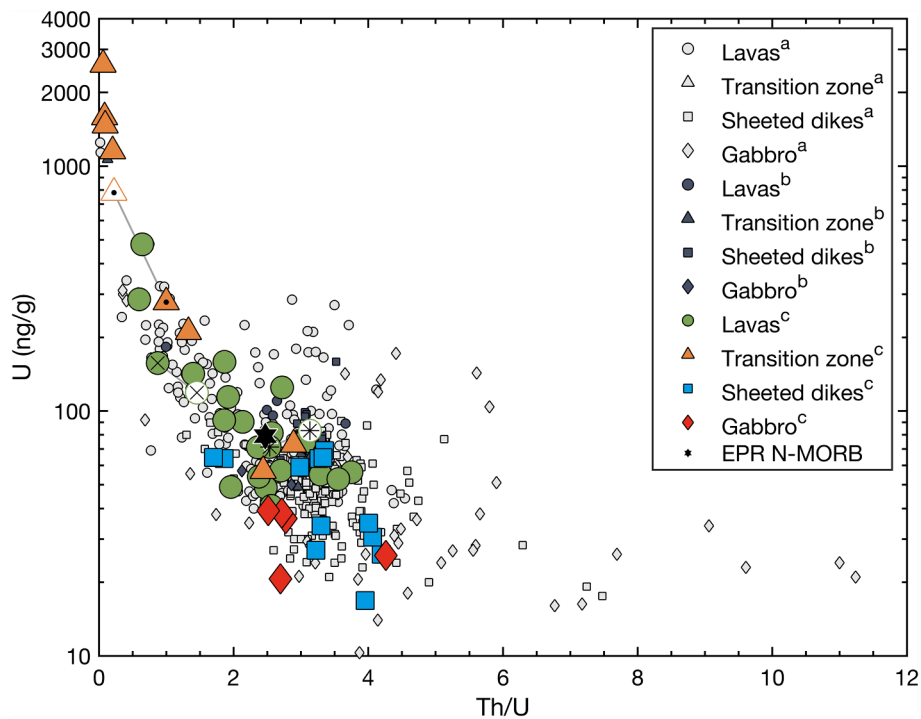
Fig. 5. Th/U ratios versus U concentrations (logarithmic scale) for all samples at Site 1256. Paired samples are linked with tie-lines; coloured and filled = halo and clast; white and hollow = background and breccia, X = 26R; ✱ = 62R; ● = 122R. In legend; 'transition zone' refers to the lava-dike transition, 'Gabbro' refers to the plutonic gabbro-dike transition. References for superscripts in legend: (a) Harris (2011); (b) Höfig et al. (2014); (c) this study. EPR N-MORB mean is from PetDb compilation.

Table 1

Different calculations of mean U, Th concentrations, Th/U ratios and δ²³⁸U for Site 1256. The concentration estimates are from the comprehensive data set of Harris (2011), while δ²³⁸U estimates are from this paper. Estimates include overall (with or without plutonic section), each stratigraphic section, and mean integrating the length scale of each lithology section scaled proportionally with the thickness of the sections (with or without plutonic section). The estimated Th/U ratios and δ²³⁸U means have been calculated as both averages and concentrated-weighted averages.

	Section thickness (m)	N	Th (ng/g)	±SD	U (ng/g)	±SD	Th/U (g/g)	±SD	Th/U (g/g) conc. weighted	N	δ²³⁸U (‰)	±SD	δ²³⁸U (‰) weighted	±SD
Overall		462	194	112	93	165	3.0	1.3	2.1	49	−0.40	0.21	−0.37	0.21
Overall (excluding Plutonic section)		413	193	101	96	172	2.8	1.0	2.0	44	−0.41	0.22	−0.37	0.22
Lava section	754	218	216	125	117	127	2.4	0.9	1.8	23	−0.50	0.24	−0.63	0.24
Lava-Dike section (Transition zone)	57	9	189	45	502	913	2.4	1.4	0.4	9	−0.28	0.18	−0.30	0.18
Sheeted dike section	346	186	167	54	52	17	3.4	0.9	3.2	12	−0.32	0.08	−0.32	0.08
Plutonic section*	88	49	198	180	68	80	4.3	2.5	2.9	5	−0.39	0.13	−0.41	0.13
Mean of sections			200	20	113	213	2.8	0.9	1.8		−0.43	0.10	−0.51	0.15
Mean of sections (excluding Plutonic section)			200	25	116	243	2.7	0.6	1.7		−0.44	0.12	−0.52	0.18

* Thickness for Plutonic section is calculated as difference between top of section and deepest sample measured for U isotopic composition.
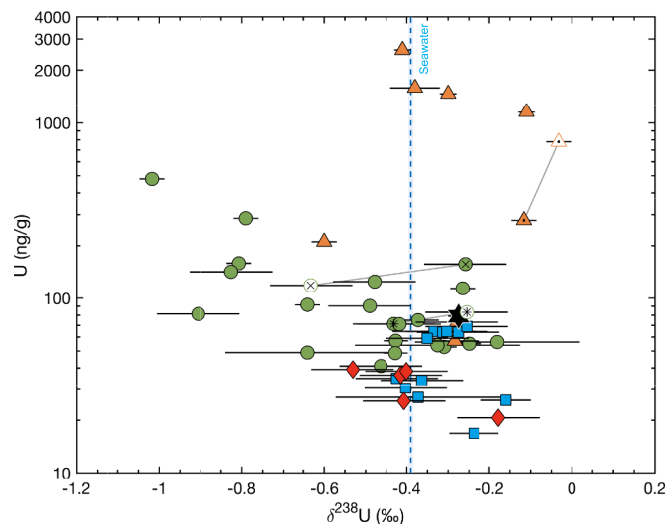
Fig. 6. δ²³⁸U compositions versus U concentrations (logarithmic scale) at Site 1256. The data has been subdivided into the four major stratigraphic sections at Site 1256 (see Fig. 4 for symbol description). Seawater δ²³⁸U is also plotted as vertical line (reference as in Fig. 2).

The extrusive lava samples (with 13 of 25 out of secular equilibrium) show δ²³⁴U generally near secular equilibrium, with the highest value of +18 ± 2 ‰ and lowest of −18 ± 10 ‰. The lava-dike transition samples show higher δ²³⁴U, up to +87 ± 5 ‰, with five of nine samples out of secular equilibrium. The sheeted dike section shows the largest δ²³⁴U variability with values up to +326 ± 6 ‰ and ten out of twelve samples out of secular equilibrium. The sheeted dike section also shows a general trend in δ²³⁴U with depth, with the highest values in the uppermost dikes (~730–850 msb) that decrease downwards in the section (Fig. 4). The plutonic dike-gabbro transition section shows δ²³⁴U both slightly above and below secular equilibrium (from −21 ± 10 to +11 ± 10 ‰) for the five samples. There are no obvious trends in a plot of δ²³⁴U versus δ²³⁸U (Fig. 7a). Comparing δ²³⁴U with U concentrations shows that, although there is no clear overall trend, samples from the lava-dike transition zone and sheeted dike sections each define a rough discrete array (Fig. 7b). In the lava-dike transition zone near the mineralised hyaloclastic breccia, samples with the higher δ²³⁴U have lower U concentrations. Similarly, samples from the sheeted dike section that yield

the highest δ²³⁴U (>100 ‰) all have U concentrations below the mean N-MORB.

5. Discussion

In the following, the processes and timing of U mobility in altered ocean crust will be discussed, focussing first on the U and Th concentrations and then the U isotope systematics in Site 1256.

5.1. Uranium mobility and source constraints from U concentrations and Th/U ratios at Site 1256

To investigate the alteration effects on U mobilisation, the protolith of unaltered mid-ocean ridge basalts at Site 1256 is an important reference point for comparison. Based on diagnostic geochemistry and radiogenic isotope ratios, the unaltered protolith material at Site 1256 reflects typical N-MORB (e.g. Höfig et al., 2014). There are a range of methods to estimate the unaltered protolith; one option is to use the least altered samples within a sample-set, following past practice (e.g. Staudigel, 2014), while using large data compilations is another option. Establishing a reference within a sample-set may be advantageous for site-specific compositions, but it is problematic at Site 1256 given the evidence for U mobility in all sections of the ocean crust sampled (e.g. variable Th/U and δ²³⁴U, Figs. 4 and 5). Global compilations of MORB samples (Gale et al., 2013; Jenner and O'Neill, 2012) yield mean Th/U ratios (~2.9 g/g) and U concentrations (~70 ng/g, see Table 2) slightly lower and higher, respectively, than the average sheeted dikes and dike-gabbro transition at Site 1256 (Table 1). Refining the possible protolith to compiled Pacific N-MORB glasses with ICP-data (best suited for reliable trace metal analyses of Th and U) from the PETDb database yields a mean Th/U ratio of ~2.5 g/g and U concentration ~79 ng/g (Table 2). In comparison, a small well-characterised data-set of Pacific N-MORB glasses screened for alteration, with δ²³⁴U in secular equilibrium (Andersen et al., 2015) gives a mean Th/U ratio of ~2.5 g/g and U concentration of ~49 ng/g (Table 2). There is a significant range in both Th/U and U concentrations depending on the data-set chosen; the variation probably reflects the combined effects of sample heterogeneity, analytical uncertainties and possible minor alteration. Given the variable Th/U ratios and U concentrations from the different compilations (Th/U ratios from 2.5 to 2.9 g/g and U concentrations from 50 to 80 ng/g), only relatively large changes from a protolith may be confidently identified in Site 1256 samples. Further reasons for caution when using Th/U ratios and/or U concentrations in samples for estimating U
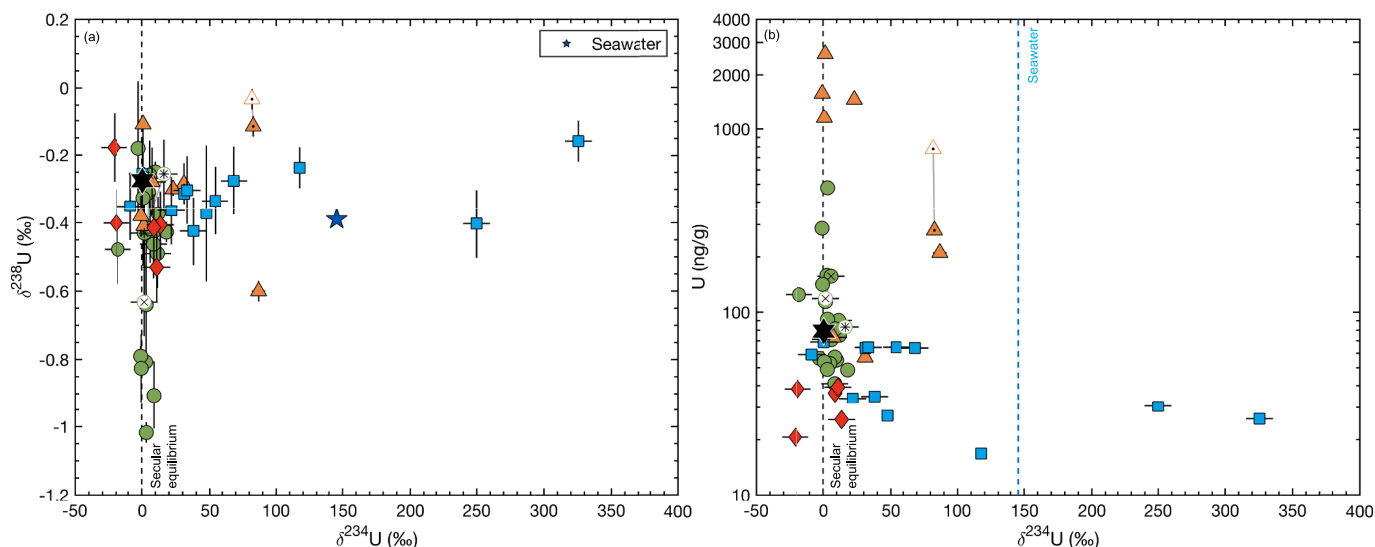
Fig. 7. (a) $\delta^{234}U$ versus $\delta^{238}U$ compositions of Site 1256 samples. Mean seawater composition and Pacific N-MORB are plotted as blue and black filled stars, respectively. (b) $\delta^{234}U$ composition versus U concentration (logarithmic scale) at Site 1256. The $\delta^{234}U$ compositions of seawater and secular equilibrium are plotted as lines (reference as in Fig. 2) whereas Pacific N-MORB are plotted as a black star. The data symbols are the same as Fig. 4.

Table 2

The mean U concentrations and Th/U ratios for different MORB compilations from either East Pacific Rise (EPR) or global coverage.

Source	N	U (ng/g)	Th/U (g/g)
East Pacific Rise (EPR)			
Andersen et al. (2015)	7	49	2.50
PetDB – Glass	807	79	2.47
PetDB – Whole rock	479	120	2.37
Global			
Jenner and O'Neill (2012)	438	66	2.94
Gale et al. (2013)	1653	73	2.84

gain/loss includes; changing sample mass can change the U concentration and the assumption that U is mobile and Th is immobile in the fluid-generating process may not be valid given the potential of significant hydrothermal Th fluid mobility under certain geochemical conditions (e.g. Nisbet et al., 2019). However, general inverse correlation between U concentrations and Th/U ratios at Site 1256 (Fig. 5) shows changes which attest to U loss/gain to first order.

Both the extrusive lavas sequence and the lava-dike transition zone at Site 1256 show evidence for overall moderate to high U additions from their elevated U concentrations and lowered Th/U ratios (Table 1), although, some extrusive lava samples have high Th/U ratios (up to ~5) at low [U] which we attribute to U loss (Fig. 5). There are features in the U concentrations in the ~750 m thick extrusive lavas that are consistent with other altered ocean crust sections. The overall significant U enrichments are similar to observations from younger ocean crust, such as from the ~6 Ma Pacific Hole 504B (Bach et al., 2003) and ~8 Ma IODP Site U1382/U1383 in the Atlantic (Türke et al., 2015), both of which show significant U enrichment compared to N-MORB in the upper ~500 m (Fig. 1), associated with secondary Fe-oxyhydroxides, clay minerals and altered glass. The U addition in the upper extrusive lava sections at Site 1256 show a weak overall trend with depth, with the greatest U enrichment in samples near the top and decreasing with depth (Fig. 4). Overall, it suggests an irregular addition of U from low-temperature seawater-derived, recharging fluids, with more U addition towards the upper parts of the Site 1256 basement.

In the plutonic dike-gabbro transition and deeper sheeted dikes at Site 1256, there is evidence for depletion of a range of elements (e.g. Cu, Zn and Pb), with enrichments of these in the upper sheeted dike and

lava-dike transition, likely via high-temperature alteration and leaching and hydrothermal fluid transport upwards and precipitation with sulfides (e.g. Alt et al., 2010; Patten et al., 2016). Although there are high U enrichments in the lava-dike transition, there are no evidence of U additions in the upper sheeted dikes (Fig. 3). The U concentration and Th/U ratio systematics in the dike-gabbro and sheeted dike sections show clear evidence for some U mobility, particular in the deeper plutonic sections with highly variable Th/U ratios from >10 to <1, although the average U concentration (~68 ng/g) and concentration-weighted mean Th/U ratio (~2.9 g/g) for the dike-gabbro section are very close to the compiled fresh N-MORB range, with no evidence of any overall U loss or gain (Fig. 3 and Table 1). The apparent U mobility and redistribution may be linked to the moderately dipping intrusive margins between the sheeted dikes and gabbros that have guided hydrothermal fluid flow and alteration in this section (Alt et al., 2010).

The sheeted dike section is on average, slightly lower in its mean U concentration (~52 ng/g) and higher in the mean concentration-weighted Th/U ratio (~3.2 g/g) than the defined fresh N-MORB range, indicating some potential U loss. This U mobility does not seem to follow the redistribution of other elements (e.g. Cu, Zn, Pb) from the dike-gabbro into the upper sheeted dike and lava-dike transition zone. Instead, some U loss in the upper sheeted dikes (from 830 to 850 msb) may have redistributed into the lava-dike transition zone. At Hole 504B, U loss from hydrothermal-fluid leaching processes has been suggested for the low U concentrations and high Th/U ratios in the sheeted dikes, whereas the lava-dike transition zone shows moderately elevated U concentrations (up ~150 ng/g; Fig. 1) and only moderately elevated $^{87}Sr/^{86}Sr$ ratios compared to pristine MORB (Bach et al., 2003; Höfig et al., 2014; Teagle et al., 1998) suggesting a dominantly U enrichment from the hydrothermal-fluid leaching of U in the sheeted dikes at Hole 504B. At Site 1256, however, the lava-dike and the upper sheeted dike section have been affected by both alteration from upwelling high-temperature and downwelling low-temperature seawater-derived hydrothermal fluids (Alt et al., 2010). The latter is evidenced from $^{87}Sr/^{86}Sr$ ratios that are strongly elevated from EPR MORB (although still significantly lower than 15 million year old seawater) and precipitation of both anhydrite and sulfide phases (Alt et al., 2010; Harris et al., 2015).

Strong U enrichment has occurred in the hyaloclastic breccia of the Site 1256 lava-dike transition (Fig. 3). The ultimate source of the U enrichment within the hyaloclastic breccia could be either basalt-

derived or seawater-derived, or perhaps, a combination of both. The hyaloclastic breccia samples in the lava-dike transition that have $^{87}Sr/^{86}Sr$ ratios (0.7052–0.7061) above the estimated ratios for black smoker fluids at Site 1256 (0.7050–0.7053: Harris et al., 2015) also include the samples with the greatest U additions (210 up to 2599 ng/g). These U concentrations are up to an order of magnitude higher than observed in the transition zone of Hole 504 (Fig. 1). This combination of high U concentrations and seawater-derived, fluid-driven alteration, suggest seawater is the dominant source for the U addition to these samples.

The transition zone at Site 1256 represents a change to a more reducing environment at depth in the altered crust and includes early, near-axis precipitation of sulfide phases from high-temperature hydrothermal alteration. This may provide the conditions for 'roll-front' U uptake (e.g. Cuney, 2010) with an oxidised seawater-derived recharging fluid transporting U^{+6} to the lava-dike transition zone where U precipitate as U^{+4}. If such a recharging fluid were to migrate further and deeper into the sheeted dikes below, it would be depleted in U from this prior removal. This behaviour could account for the high U addition in the lava-dike transition and the limited U addition observed in the upper sheeted dikes, despite the evidence of seawater-derived fluid interaction in both areas. The specific form of the U uptake in the lava-dike transition zone is unknown, yet typical phases associated with roll-front U uptake includes precipitation of reduced U oxides species such as uraninite (e.g. Cuney, 2010), whereas carbonates precipitated under reducing conditions may contain high U concentrations (e.g. Israelson et al., 1997). It is also worth noting that the mechanisms of U uptake from a seawater-derived fluid into altered ocean crust, may differ from those of other elements such as Rb uptake or Sr exchange, and, thus, correlations are not necessarily expected between different elements. Further discussion for the uptake mechanisms and timing of the U mobility at Site 1256 based on U isotopes is considered in the next sections.

5.2. Uranium mobility estimates from $\delta^{238}U$ at Site 1256

Changes in $\delta^{238}U$ may be used to further evaluate the U sources and mobility within Site 1256. The protolith $\delta^{238}U$ may be estimated from the pristine Pacific N-MORB glasses (with $\delta^{234}U = 0$) from Andersen et al. (2015) giving -0.28 ± 0.03 ‰ (2SD, n = 7). There are samples deviating from the protolith composition in all the sections within Site 1256.

5.2.1. $\delta^{238}U$ in the extrusive lavas

The extrusive lava section displays an irregular distribution of $\delta^{238}U$ values ranging from measurements similar to mean Pacific N-MORB towards lower values (Fig. 4). The $\delta^{238}U$ show limited correlation with observed alteration in the samples. For instance, the two sets of paired 'halo' and 'fresh' counterparts (190 and 437 msb) show no systematic changes in the $\delta^{238}U$ nor U concentrations. At 190 msb, the sample with the lowest $\delta^{238}U$ (-0.62 ‰) is in the 'background' alteration, whereas at 437 msb it is the 'halo' that shows the lowest $\delta^{238}U$ (-0.43 ‰) of the sample pairs. Also, the two samples from the highly altered 'red brick horizon' (~398 msb) yielded $\delta^{238}U$ close to seawater (both $-0.43 \pm$ 0.03 ‰) and U concentrations (~50 ng/g) and Th/U ratios (~2.6 g/g) close to mean Pacific N-MORB. It has been suggested that the 'red brick horizon' was likely altered by conductively cooled upwelling hydrothermal fluids (Gao et al., 2012; Harris et al., 2015). If the case, perhaps some U exchange process has occurred with hydrothermal fluids and the $\delta^{238}U$ close to seawater is coincidental. Other samples with U enrichments and $\delta^{238}U$ near to mean Pacific N-MORB and seawater, may be from near-quantitative uptake of seawater-derived U or U uptake with limited isotope fractionation. A lower, but muted, $\delta^{238}U$ is the expected direction for $^{238}U/^{235}U$ fractionation occurring with U exchange in the U^{+6} oxidation state, as observed in low-temperature U adsorption experiments and in marine ferro-manganese deposits (e.g. Goto et al.,

2014; Jemison et al., 2016).

Another explanation for U addition with low $\delta^{238}U$ may be U uptake from an evolving fluid carrying low $\delta^{238}U$, from prior partial U removal with a high $\delta^{238}U$. Correlations between decreasing $\delta^{238}U$ and decreasing U concentrations has been observed in evolving fluids and solids downgradient in sandstone-hosted U roll-front redox systems, with prior U^{+4} precipitation with high $\delta^{238}U$ (Basu et al., 2015; Murphy et al., 2014). In contrast, the samples in the extrusive lava section with the lowest $\delta^{238}U$ are characterised by the highest U concentrations, showing systematics in the opposite direction. Thus, the more likely scenario is partial U uptake from an oxidised low-temperature recharging seawater-derived fluid and U isotope fractionation towards lighter values. The strong U ppm-level enrichment involving secondary Fe-oxyhydroxides in other extrusive sections of altered ocean crust and sediments (Mills and Dunk, 2010; Türke et al., 2015) suggests, this could be a likely secondary phase for significant U addition. Also, marine and terrestrial alteration of serpentinites show strong U enrichments which correlates positively with increasing Fe^{3+} over total Fe (Pavia et al. 2023), suggesting U addition with Fe-oxyhydroxides. The altered serpentinites have $\delta^{238}U \sim 0.2$–0.3 ‰ lower compared to protolith samples (Pavia et al., 2023) a similar lowering of $\delta^{238}U$ as seen in marine ferromanganese deposits compared to seawater (e.g. Goto et al., 2014). Lowering of $\delta^{238}U$ on the ~0.2 ‰ level, is also consistent with experimental result from U adsorption on goethite and birnessite (Brennecka et al., 2011; Jemison et al., 2016).

A lowering of $\delta^{238}U$ on the 0.2–0.3 ‰ level compared to the protolith or the seawater value is within a range of the $\delta^{238}U$ of extrusive lavas with elevated U, however, some samples are significantly lower (e.g. sample 16R-1 88–95 at 120 msb at -1.02 ‰). This shows that U uptake in some of the altered oceanic crust samples at Site 1256 is not dominated by the same U equilibrium uptake mechanism as within ferromanganese deposits. The samples at Site 1256 with the lowest $\delta^{238}U$ (<-0.80 ‰) all display 'background' alteration style (Harris et al., 2015). However, some background alteration samples have higher $\delta^{238}U$, and so this alteration style is not definitively diagnostic. The very low $\delta^{238}U$ could possibly be linked with multi-stage U uptake during adsorption associated with secondary phases or driven by kinetic a/biotic processes within the hydrothermal systems in the upper portion of the altered ocean crust. Further work to understand the U uptake mechanisms responsible for these low $\delta^{238}U$ in the samples are needed.

5.2.2. $\delta^{238}U$ in the Lava-dike transition zone

The upper, basalt-dominated samples in the lava-dike transition zone show no evidence of significant U uptake, whereas the hyaloclastic breccia samples below show greatest U additions and includes the highest $\delta^{238}U$ (-0.03 ± 0.02 to -0.60 ± 0.03 ‰) and most elevated $^{87}Sr/^{86}Sr$ ratios of all whole rock samples at Site 1256. As with the U concentrations, there is no clear relationship between the $^{87}Sr/^{86}Sr$ ratios and the $\delta^{238}U$ (Fig. 8). The high $\delta^{238}U$ could be from an evolving seawater-derived fluid which has precipitated U with isotopically light U prior in the extrusive lava section, however, the very high U concentrations in these samples makes this scenario unlikely.

Focussing on the samples in the central hyaloclastic brecciated zone, the two samples with the highest U concentrations have $\delta^{238}U$ ($-0.41 \pm$ 0.03 and -0.38 ± 0.06 ‰) within the compositional range of modern seawater, whereas the samples with lower U concentrations have higher $\delta^{238}U$ (Fig. 6; 777–779 msb). This is consistent with an overall pattern of U isotope fractionation towards higher $\delta^{238}U$ moving from partial (lower U concentration samples) to near-quantitative (higher U concentration samples) U uptake. The overlap with seawater $\delta^{238}U$ in the highest U concentration samples, again supports seawater-derived U as the dominant source of U added to these samples. As discussed above, the more reducing environment at the lava-dike transition makes a roll-front U removal scenario plausible. This is supported by the elevated $\delta^{238}U$ in hyaloclastic samples, as observed in other roll-front U precipitates (e.g. Basu et al. 2015; Murphy et al., 2014). Potential host phases for such U
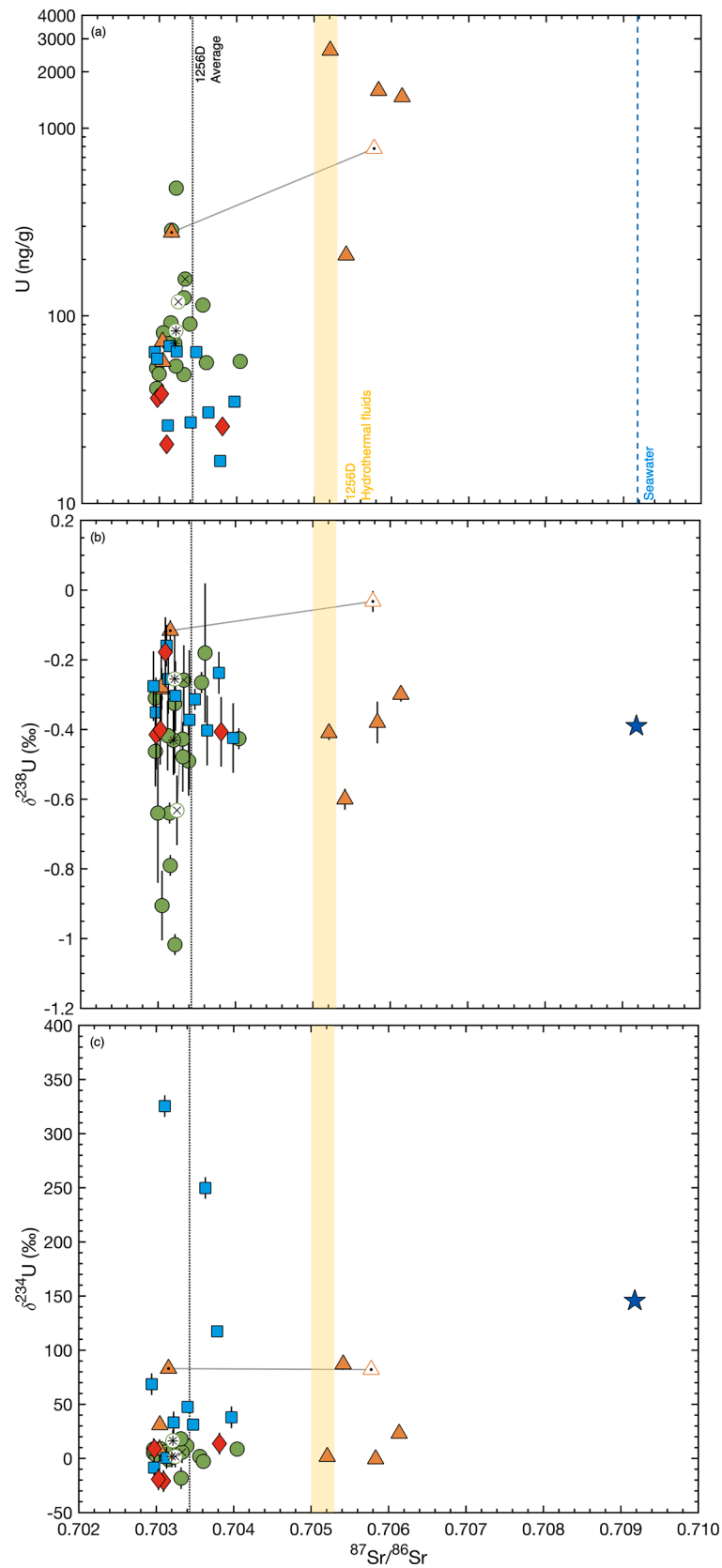
Fig. 8. $^{87}Sr/^{86}Sr$ ratios vs. U concentrations (a), $\delta^{238}U$ (b) and $\delta^{234}U$ compositions (c) at Site 1256 (note U is on a logarithmic scale). The data symbols are the same as Fig. 4, but additionally include 1256 hydrothermal band (yellow band) and seawater composition (blue band or star). The $^{87}Sr/^{86}Sr$ ratio data are from Harris et al. (2015).

addition could be U oxides or other U^{+4}-bearing phases and calcite precipitates under reducing environments which generally show elevated $\delta^{238}U$ (e.g. Bopp et al., 2009; Romaniello et al., 2013). A modelled U isotope fractionation evolution for the fluid and precipitates is in principle possible, however, it is limited by the difficulty of estimate the total U fraction from the fluid added to each of the samples.

In contrast, the deepest lava-dike transition sample measured in the hyaloclastic breccia with sheeted dike clasts at 782 msb has a lower (although elevated) U concentration (210 ng/g) and a lower $\delta^{238}U$ (-0.60 ± 0.03 ‰) than the hyaloclastite samples above (Fig. 4). This sample also has an elevated $^{87}Sr/^{86}Sr$ ratio (0.7054) indicating some seawater-sourced Sr. If this sample is considered in the context of a U roll-front system, where the main area of U uptake is in the hyaloclastic zone above, this sample is below the main U mineralisation zone. The low $\delta^{238}U$ in this sample then fits with a scenario of precipitation of U^{+4}-bearing phases above, making the fluid low in $\delta^{238}U$, in a similar way as measured $\delta^{238}U$ in downgradient fluids samples following reductive U removal in sandstone-hosted U roll-front deposits (e.g., Basu et al., 2015; Murphy et al., 2014).

5.2.3. $\delta^{238}U$ in the sheeted dikes and plutonic dike-gabbro sections

In the plutonic dike-gabbro section, the sample with the lowest U concentrations (21 ng/g), shows the highest $\delta^{238}U$ (-0.18 ± 0.10 ‰) similar to the mean Pacific N-MORB, whereas the other four samples, also with low U (26–39 ng/g), have $\delta^{238}U$ (-0.40 ± 0.10 to -0.53 ± 0.10 ‰) below the mean Pacific N-MORB. This suggests some, but limited, changes in $\delta^{238}U$ during the U mobility and redistribution in the dike-gabbro transition section. The sheeted dikes also show limited variation in $\delta^{238}U$, with nine out of twelve samples with $\delta^{238}U$ similar to the mean Pacific N-MORB, with two slightly below (-0.42 ± 0.10 and -0.40 ± 0.10 ‰) and one slightly above (-0.16 ± 0.06 ‰) (Fig. 4). If the low U concentrations in the upper part of the sheeted dikes are due to U leaching and loss, it suggests limited U isotope fractionation during this process. The upper sheeted dike section shows precipitation of both anhydrite and sulfide phases (Alt et al., 2010) yet this appears not to be accompanied by significant U uptake. If the anhydrite mineralisation is mainly from a seawater-derived fluid the limited U uptake could be due to the fluid have lost most of the U prior at shallower depth, either via U^{+6} adsorption in the extrusive lava section or as U^{+4} across a redox front in the lava-dike transition section. However, despite the low U, the high $\delta^{234}U$ values for some samples in the upper sheeted dikes are consistent with some U uptake. Thus, it is possible that several different mechanisms for U mobility, with different timings, have contributed to the overall U systematics observed. This will be explored further using the $\delta^{234}U$ systematics in Section 5.3.

5.3. Uranium mobility and sources estimated from $\delta^{234}U$ at Site 1256

The measured $\delta^{234}U$ at Site 1256 suggest that the timing of the U addition is complex, as samples with evidence of U addition and loss display $\delta^{234}U$ within and significantly out of secular equilibrium. There is no trend in $\delta^{238}U$ versus $\delta^{234}U$ (Fig. 7a), suggesting that U mobility has occurred both prior to, allowing the $^{234}U/^{238}U$ ratios to return to secular equilibrium, and within the last ~1.5 million years. The $\delta^{234}U$ values furthest from secular equilibrium are within the lava-dike transition and particularly in the sheeted dikes, with two samples ($+327 \pm 10$ and $+250 \pm 10$ ‰) above the modern seawater value of ~$+145$ ‰ (Fig. 4). A potential explanation for the excess ^{234}U is a seawater contaminant during drilling, however, this is an unlikely scenario given the $\delta^{234}U$ higher than the seawater value in some samples and that $\delta^{234}U$ disequilibrium was measured in samples that were cored during different drilling expeditions (Leg 206, 309 and 312; Fig. 4). Instead, the significant disequilibrium in $\delta^{234}U$ is evidence for the 'recent' (here used for the last 1.5 million years) mobility of U at hypabyssal levels of the ocean crust at Site 1256. Previous observations of fresh versus altered pillow lavas and drilled shallower ocean crust have shown $\delta^{234}U$ mainly

between secular equilibrium (0 ‰) and modern seawater ($+145$ ‰), but with a few samples falling outside this range, with both higher and lower $\delta^{234}U$ values, to the level quantifiable with low precision alphas counting techniques (Bacon, 1978; Macdougall et al., 1979). Also $\delta^{234}U$ values higher than the seawater value have been observed from U addition in weathered serpentinites (terrestrial and marine) and altered ocean crust, pointing to U addition from a seawater-derived hydrothermal fluid source with further elevation of $\delta^{234}U$ from leaching recoiled ^{234}U along fluid pathways (Pavia et al., 2023; Reyss et al., 1987).

The very high $\delta^{234}U$ values in some samples at Site 1256 are associated with relatively low U concentrations (~26 and ~31 ng/g) from the uppermost sheeted dikes, while elevated, but lower $\delta^{234}U$ occur in samples stratigraphically above and below (Fig. 4). The overall trend in the sheeted dikes with high $\delta^{234}U$ in the upper part (~777 to 850 msb) and decreasing with depth, could potentially be explained by upwelling of basalt-derived fluids, rather than downwelling of seawater-derived fluids. However, the ~15 Ma age and progressive cooling of the ocean crust makes recent high-temperature hydrothermal activity unlikely. Also, a positive correlation between $\delta^{234}U$ and U concentrations would be expected from this scenario, yet is not observed; samples from the overlying lava-dike transition have higher U concentrations but lower $\delta^{234}U$ (up to $+87 \pm 5$ ‰).

Instead, the samples with $\delta^{234}U$ above secular equilibrium in Site 1256, are likely to have experienced U uptake via precipitation from a low-temperature seawater-derived fluid, with modified $\delta^{234}U$ from ^{234}U leaching of alpha-recoil damaged sites in the ocean crust rock matrix along the fluid pathway (leaving those conduits depleted in ^{234}U). The downward migration of such a seawater-derived fluid could have precipitated most of the U at the hyaloclastic breccia with the redox transition and leaving a modified fluid, with lower U concentration, to migrate further below into the sheeted dikes. As discussed, some samples in the upper part of the sheeted dikes have very low U concentrations (<30 ng/g) likely from U loss during hydrothermal alteration at greenschist facies conditions at an early stage near the ridge axis. Therefore, given the low U concentrations, even minor recent U additions with a high $\delta^{234}U$, will have a large impact on the bulk $\delta^{234}U$ value of the sample. Such a scenario is broadly consistent with the pattern of generally higher $\delta^{234}U$ with lower U concentrations for samples both in the lava-dike transition and sheeted dike intervals (Fig. 7b).

Based on the $\delta^{234}U$ data, a sensitivity exercise can be done to estimate the relative fraction of recent U uptake compared to the total U in the sample. Assuming the measured $\delta^{234}U$ in the samples is a mixture between recent U uptake from a fluid with a high $\delta^{234}U$ and older U (>1.5 Ma) with $\delta^{234}U = 0$ ‰, the relative contribution of the recent U uptake can be estimated. This calculation can be done for all samples with $\delta^{234}U > 0$ ‰ if the $\delta^{234}U$ of the fluid is known (all normalised to present-day compositions from the radioactive decay of the U isotopes). In the study of Pavia et al. (2023), the fluid adding excess U during the seawater-alteration of marine serpentinites had an estimated $\delta^{234}U$ of ~589 ‰. Using a similar $\delta^{234}U$ for the U in the fluid (600 ‰), 'recent' U addition from this fluid was estimated for the samples measured at Site 1256 (Supplementary Table 3). This estimate shows only minor recent U contributions (below 4 ng/g U and below 4 % addition) for the shallow extrusive lavas and deep plutonic dike-gabbro transition samples, that show little disequilibrium in $\delta^{234}U$. For some samples in the lava-dike transition and sheeted dike sections, the changes are more significant. In the high U-containing samples in the hayloclastic breccia, recent U addition contributes up to ~100 ng/g, a maximum 14 % recent U addition compared to the total U inventory. In the sheeted dikes, the calculated recent U addition is also significant for the samples with high $\delta^{234}U$, with up to 14 ng/g U addition that contributes up to 52 % of the total U.

There are some obvious sources of uncertainty with these estimates of recent U addition, including that the fluid $\delta^{234}U$ may be variable and/ or different from the value used here. Using a higher $\delta^{234}U$ in the fluid,

the recent U addition estimates would decrease, whereas using a lower δ^{234}U the estimates would increase. However, a significantly lower fluid δ^{234}U would imply some samples were extremely depleted in U prior to recent addition, as the calculated recent U addition already contributes up to 52 % of the total U in some samples with low bulk U (26–39 ng/g) and we consider this unlikely. This simple calculation approach shows that U uptake from recent seawater-derived fluid with a high δ^{234}U may have a significant impact on the δ^{234}U compared more limited effects on the U concentration for most samples. Although the highest δ^{234}U is in the samples from uppermost sheeted dikes, the calculated total amount of recently added U is up to eight times higher in the hyaloclastic breccia than in the lava-dike transition samples. These observations point to a seawater-derived fluid active during the last 1.5 my being channelled through and reacting with the deeper parts of the Site 1256, with U uptake at the redox change in the lava-dike transition, perhaps via a similar mechanism as the U uptake that occurred prior to the last 1.5 my.

The δ^{234}U data also suggest that a range of the sheeted dikes samples experienced recent U addition. However, the overall low bulk U concentration and Th/U ratios point to an overall U depletion, suggesting that these samples were previously even more depleted in U. Using the estimated recent U addition, the samples Th/U ratios prior to this addition may be estimated by subtracting the recent from the bulk U concentration (Supplementary Table 3). The estimated Th/U ratios prior to the recent U addition for the two sheeted dike samples with the δ^{234}U above the seawater value, changed significantly to 9.2 and 7.0 (from 4.2 and 4.1, respectively). Although these Th/U ratios estimates are lower than any measured bulk samples in the sheeted dike section, they are within the lower Th/U ratios measured in the plutonic dike-gabbro transition (Fig. 5), a region with little evidence for recent U addition, making the U losses of these samples within reasonable bounds. Why these upper sheeted dike samples first experienced U loss followed by recent U addition, may be related to the pathways of fluids and timing of the U addition (see further discussion in Section 5.4).

Lastly, the calculations for recent U addition using the δ^{234}U, can also be extended to include an estimate of the δ^{238}U of the sample prior to recent U addition, if the δ^{238}U of the U-carrying fluid is known. Again, there are several complexities here, particularly, whether the U addition from a fluid is invoked with or without an expressed U isotope fractionation (e.g. quantitative vs. non-quantitative U addition) and exact U isotope fractionation factors for the U uptake processes. Thus, calculated δ^{238}U in the samples prior to recent U addition, should be considered as a measure of sensitivity to the potential impact of the recently added U on the δ^{238}U of the sample. Assuming a δ^{238}U for the U in the fluid of either −0.60 or −0.03 ‰, the highest and lowest δ^{238}U measured in the lava-dike transition and sheeted dike section, and assuming no U isotope fractionation during the U addition process, the δ^{238}U for the samples prior to the recent U addition, can be estimated (Supplementary Table 3). Using −0.60 or −0.03 ‰ as end-members for δ^{238}U in the fluid, only the two samples with the highest δ^{234}U show significant change of >0.1 ‰ in the δ^{238}U. These two samples show estimated maximum δ^{238}U changes of up to 0.52 ‰ higher and 0.27 ‰ lower than the bulk samples δ^{238}U. For most samples, similar to the U concentrations, the changes in δ^{238}U are generally of little significance despite the changing δ^{234}U, again showing the larger leverage changes in δ^{234}U typically have compared to δ^{238}U and U concentrations.

5.4. Generalised uranium isotope evolution in the altered ocean crust at Site 1256

By combining observations of hydrothermal conditions and distribution of alteration products (Alt et al., 2010; Teagle et al., 2006) with the U systematics discussed in the previous sections, it is possible to evaluate the evolution of U mobilisation and uptake in upper ocean crust formed at a fast spreading rate. Thus, we add the U systematics to the stages of alteration suggested by Harris et al. (2015). The first alteration stage is near the ridge axis with high-temperature greenschist facies

alteration in the sheeted dikes and dike-gabbro transition (Alt et al., 2010). The magmatic-driven hydrothermal circulation led to metal leaching in the sheeted dikes and gabbro sections with precipitation of metal sulfides (mainly pyrite) near the top of the sheeted dikes and in the lava-dike transition (Alt et al., 2010; Patten et al., 2016). These reactions appear to have resulted in only minor localised hydrothermal leaching and re-distribution of U in the sheeted dikes and dike-gabbro transition, possibly with minor addition of U in the lava-dike transition (Figs. 4 and 5). There is little evidence for net U excess in the sheeted dike and dike-gabbro transition, and therefore, little evidence for significant high-temperature near-axis quantitative U uptake at depth in this ocean crust, as would be estimated from measurements of low-U fluids at black smoker vents (Chen et al., 1986; Michard et al., 1983; Mottl et al., 1998). It may be that U uptake occurs during low temperature processes at shallower depth in diffuse, downwellings that feed higher temperature systems at greater depth, or that on-axis U uptake is of less significance from an U uptake mass-balance perspective. The on-axis precipitation of hydrothermal reductive phases (e.g. metal sulfides) would have provided an upwards shift in reducing conditions to just below the lavas section.

The migration of the ocean crust away from the ridge axis led to more extensive low-temperature alteration of the lavas by seawater-derived ridge flank hydrothermal fluids (Alt et al., 2010). The uptake of U off-axis is evidenced by the alteration and U uptake in the upper lava pond that cooled and solidified a short distance (~10 km) off-axis (Harris et al., 2015; Teagle et al., 2006). The off-axis low-temperature alteration led to significant U uptake under largely oxidised conditions characterised by low δ^{238}U from U^{+6} adsorption or incorporation processes. At depth in the lava-dike transition section, deep channelling of seawater-derived fluids may have provided transport of U to be precipitated as U^{+4}-bearing phases, including high δ^{238}U across a redox front as an U roll-front type uptake in the lava-dike transition zone.

The δ^{234}U data shows that the ~15 million old Site 1256 has experienced U mobility within the last ~1.5 years. The slightly positive δ^{234}U values of some extrusive samples indicates recent channelled flow of seawater-derived fluids in the uppermost basement. While the recent U addition to the extrusive section is minor, there is significant U uptake in the deeper lava-dike transition zone and within the sheeted dikes. The high δ^{234}U values in the lava-dike transition zone and sheeted dikes (with extreme values in the uppermost sheeted dikes) are likely derived from the passage of seawater-derived fluids with additional ^{234}U from preferential leaching along the fluid pathways. The U uptake within the sheeted dikes, appears to have mainly been from this recent phase of U uptake and mobility. Although speculative, samples with previous U removal in the sheeted dikes may have mineralogy favouring, this later U uptake, compared to less altered samples within the sheeted dikes, e.g. via adsorption to chlorite, an abundant secondary phase in these samples (Alt et al., 2010).

The evidence for recent U mobilisation at hypabyssal depths in at Site 1256 is surprising as the hydrologic situation at the site is quite different to some other sites from the eastern Pacific (e.g., Site 504B; EPR; Juan de Fuca Ridge) where the sections show significant faulting and basement topography, and/or are only thinly sedimented and show advective heat flow and pore water chemical gradients that provide clear evidence for on-going low-temperature flow of seawater-derived fluids (e.g., Fisher et al., 1994; Kuhn et al., 2017). At Site 1256, the thick sediment cover (>250 m) and smooth basement topography indicates that recharge vertically through the sediment cover is unlikely as evidenced by the diffusive temperature and sediment porewater gradients (Alt et al., 2010; Teagle et al., 2012). However, inflections in wireline temperature profiles measured in Hole 1256D indicate zones of elevated porosity and on-going lateral fluid flow in the lower lavas (~670 msb) and the top of the sheeted dikes (805 msb, see Teagle et al., 2006, 2012). Generally low heat flow on the Cocos Plate and the presence of extinct hydrothermal pits in the region of Site 1256 have been interpreted as discharge sites for "hydrothermal siphons" where cold seawater flowed into the ocean

crust via seamounts that punctured the sediment cover (Villinger et al., 2017). There are seamounts rising to hundreds of meters above the surrounding abyssal plains ~20 km to the north-east of Site 1256 as well as a number of smaller features on the region. Although the hydrothermal pits studied to date are not sites of active fluid venting there may still be structures in the region that facilitate the recent ingress of seawater into the ocean crust at Site 1256.

5.5. The U isotope signatures of altered ocean crust

The observed U mobility and $\delta^{238}U$ variations at Site 1256 are similar to previously investigated profiles of upper ocean crust. In common with Hole 504B (Bach et al., 2003; Höfig et al., 2014), Site 1256 shows only limited U uptake, if any, in the lower sheeted dikes (and gabbros) that may be attributed to high-temperature hydrothermal circulation at the mid-ocean ridge axis (Figs. 1 and 4). The general U uptake with low $\delta^{238}U$ in the upper extrusive lava section at Site 1256 is similar to observations in the upper parts at Site 801 (Andersen et al., 2015; Noordmann et al., 2016). Composite samples representing the upper ~420 m of the ocean crust at Site 801, have U concentrations approximately five times higher than unaltered MORB, although $\delta^{238}U$ vary with depth (Fig. 2). The Site 801 composite sample from the uppermost section (0–110 msb) has low $\delta^{238}U$ values of ~-0.44 ‰ whereas composite samples from two deeper sections (110–220 and 220–420 msb) show significantly higher $\delta^{238}U$ values (of ~+0.16 ‰ and −0.14 ‰). The supercomposite sample that integrates the whole drilled section at Site 801 suggests average $\delta^{238}U$ of −0.17 + 0.05 ‰ (Andersen et al., 2015). The changing $\delta^{238}U$ down-hole at Site 801, suggests a change in the dominant U uptake mechanism. A typical temporal alteration sequence in altered ocean crust consists of ferric-iron bearing celadonite veins, with later Fe-oxyhydroxides and the then partial overprinting by a reduced assemblage of Mg-saponite and pyrite with interspersed carbonate veins (Alt and Teagle, 2003). This change from early oxidised to more reducing conditions later, reflects changing fluid flow pathways and more restricted connections to ocean seawater as the crust moves away from the ridge axis due to secondary minerals forming in the basalts and increasing sediment burial. Uranium enrichments are evident in breccia zones including in redox halos moving away from alteration veins, displaying roll-front redox U deposition type patterns (Alt and Teagle, 2003; Kelley et al., 2005). The $\delta^{238}U$ data implies that in the uppermost levels, the U incorporation from relatively oxidised seawater-derived fluids occurs without any significant redox change, for instance, through the adsorption on to Fe-oxyhydroxides or precipitation of carbonates, with little or isotopically light U uptake. The shift towards higher $\delta^{238}U$ in the lower sections of Site 801 suggest change from U^{+6} to U^{+4}- bearing precipitates, as the main process of U removal in the deeper sections. This pattern in the composite samples is consistent with discrete bulk rock and calcite samples at both Site 801 and 417/418 (Fig. 2).

In contrast at Site 1256, the ~750 m of lava section all show $\delta^{238}U$ consistent with oxidised U^{+6} uptake. We note that oxidation halos are much less strongly developed in the lavas at Site 1256 compared with other ocean crust sites, particularly those from slower spreading rates (see Alt et al., 2010). At Site 1256, the strongest U uptake is in the underlying lava-dike transition. As coring in Hole 1256D is only the second *in situ* sampling of the lava-dike transition (after Hole 504B), it is difficult to evaluate whether such deep U uptake is a common feature of altered ocean crust. The generally higher $\delta^{238}U$ in the lava-dike transition section compared to the extrusive lava section, likely reflect a change to more reducing character of U^{+4} uptake, as also seen at depth at Site 801.

Comparing U concentrations to $\delta^{238}U$ for samples from Sites 1256, 801 and 417/418, the combined samples exhibit roughly similar behaviours. Some samples define a trajectory of moderate U uptake under oxidised conditions and yielding rocks with low $\delta^{238}U$ (Fig. 9) Some of these samples could in principle also be from the addition of U with low

$\delta^{238}U$, although a lower U concentration would then be expected, as previously discussed. A second trend is defined by greater extents of U enrichment with high $\delta^{238}U$ indicating U uptake as U^{+4} under reducing conditions. A third trend is defined by samples with the highest U concentrations with seawater-like $\delta^{238}U$, suggesting near-quantitative U uptake from a seawater-derived fluid. A fourth trend to low U concentrations, but with $\delta^{238}U$ close to mean Pacific N-MORB, suggest U loss but with only minor isotope fractionation (Fig. 9). These combined trends suggest that similar processes for U uptake and U isotope fractionation in the altered ocean crust over the past ~170 million years, although the proportion of oxidised versus reducing U uptake is different at the different sites.

It is notable that the inferred trends in the mechanisms of U uptake, based on the isotope systematics, are not necessarily directly comparable to the overall observed geology and alteration assemblages in the different drilled sections of ocean crust. For instance, the occurrence of oxidised halos and Fe-oxyhydroxides are more common at Site 801 than at Site 1256 (Alt et al., 2010) yet oxidised U uptake is more prevalent at Site 1256 over Site 801. However, caution should be taken with broad generalisations between dominant alteration assemblages and U uptake given the very heterogeneous nature and distribution of U in altered ocean crust. Specifically, spatially restrictive reductive areas with high U^{+4} uptake may, by mass balance, outweigh large areas of lower levels of U^{+6} uptake. A mass balance consideration of the U removal from the dominantly oxidised modern ocean illustrates this, where only <1 % cover of reducing (sub-oxic to sulfidic-anoxic) sediments on the ocean seafloor are responsible for ~55 % of the U removal from the ocean (e.g. Dunk et al., 2002). For a high U uptake under reducing conditions, U-rich oxidised hydrothermal fluids are required to transport soluble U to regions of the ocean crust where U removal can occur via U^{+4} precipitation, similar to U removal in oceanic reducing sediments (e.g. Dunk et al., 2002) or redox sandstone-hosted U roll-front systems (e.g., Cuney, 2010). Thus, evidence of an abundance of oxidised alteration products in an altered ocean crust is not in itself diagnostic of dominantly oxidised U uptake. Reductive U uptake in altered ocean crust is likely to occur at different length scales, for example in metre thick zones as in mineralised hyaloclastic breccia in the lava-dike transition zone at Site 1256 or, as observed at Site 801, at cm to mm length scales with high U concentrations in redox vein halos and secondary carbonate precipitates (Kelley et al., 2005). Further research on the better characterisation of U uptake and isotope fractionation with alteration phases and products is needed.

5.6. The U budgets and isotope systematics of altered ocean crust

By combining the new analyses for Site 1256 with published data, it is possible to make a broad estimate for the typical U uptake for hydrothermally altered upper ocean crust, while acknowledging the caveat of the limited data available to make generalised estimates of a significant portion of Earth's surface (Table 3). Using the average U concentration of an estimated pristine rock protolith and subtracting this from the estimated average U concentration obtained from each location of deep-drilled, altered ocean crust, its U excess can be estimated. All the drilled sections of altered ocean crust investigated, show evidence of overall U addition across the age range and geographical cover (Bach et al., 2003; Harris, 2011; Kelley et al., 2005; Kelley et al., 2003; Mitchell and Aumento, 1977; Staudigel et al., 1996; Türke et al., 2015).

A range of young <20 million years crust (Sites 332/333, 504B, U1392/U1393, 1256) have non-ideal calculated means from averaged, measured U concentrations in discrete samples. For Site 1256 the estimate has been taken from the mean using the length-scale of the lithology sections (excluding the plutonic dike-gabbro section) (Table 1). We further note that data from Site 332/333 were not measured using modern techniques (Mitchell and Aumento, 1977) and may therefore be less reliable an estimate. However, all locations show a similar feature of moderate U enrichments (~50–150 ng/g). In contrast, the estimates for
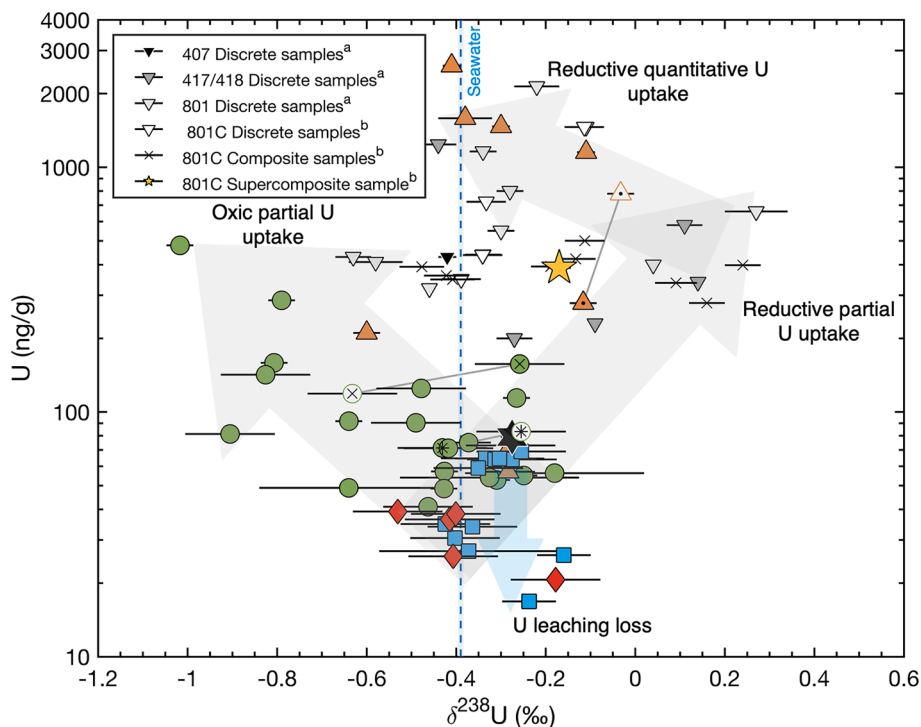
Fig. 9. $\delta^{238}U$ versus U concentrations at Sites 1256, 417/418 and 801 (note U is on a logarithmic scale). The data symbols for 1256 are the same as Fig. 4 whereas Sites 801 and 417/418 are described in the legend (see also data sources in Fig. 2). Three schematic pathways of U addition have been added to the figure as arrows of oxic partial U uptake, reductive partial U uptake and reductive quantitative U uptake. A fourth pathway is plotted suggesting U loss with little change in $\delta^{238}U$ composition (see text for discussion). Data sources (a) Noordmann et al. (2016) and (b) Andersen et al. (2015).
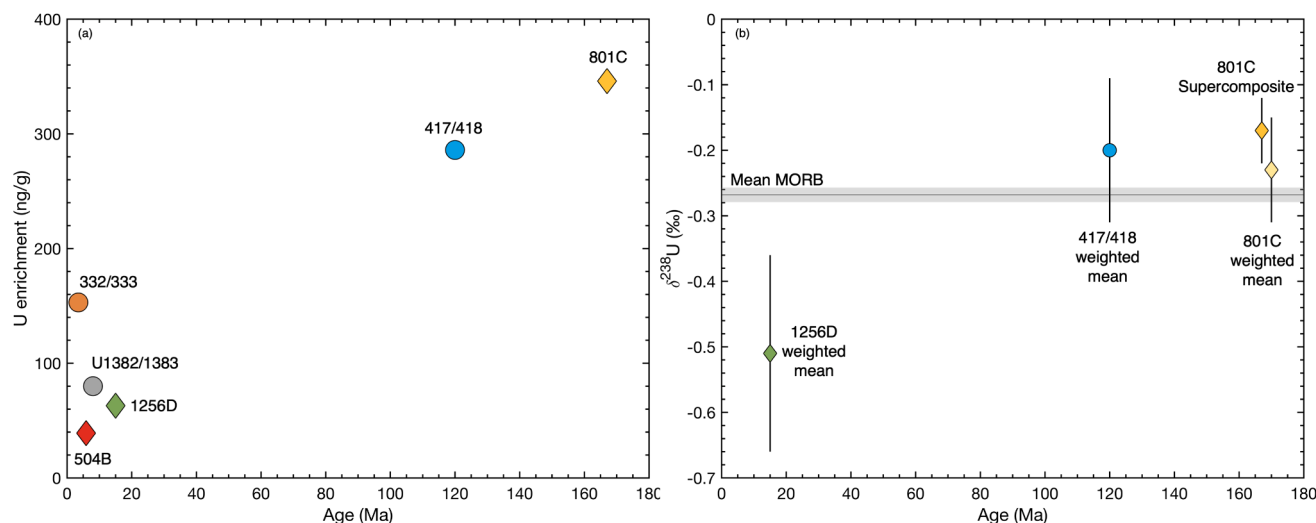
Table 3
Mean estimated U enrichments for six altered crust sites based on the U concentration in altered oceanic crust (U AOC) subtracted the estimated protolith (U MORB). The mean $\delta^{238}U$ estimates for 1256, 417/418 and 801 are based on U-weighted averages of lithology averaged $\delta^{238}U$ values (g) discrete $\delta^{238}U$ values (h,j) and based on supercomposite measurement (i). 'DIB' is depth in Basement and 'SD' is sheeted dike. Data sources: (a) Mitchell and Aumento (1977); Average AOC and MORB (MORB estimate from Site 335)/(b) Bach et al. (2003); Average AOC and MORB/(c) Türke et al. (2015); average AOC, MORB average for all Th/U > 2/(d) Harris (2011) average AOC and MORB/(e) Staudigel et al. (1995), Staudigel et al. (1996), Kelley et al. (2005); average AOC from composite and MORB average from Site/(f) Kelley et al. (2003), Kelley et al., (2005); average AOC from composite and MORB average from Site/(g) this study; $\delta^{238}U$ data, ±1SD/(h) Noordmann et al. (2016); $\delta^{238}U$ data, ±1SE/(i) Andersen et al., (2015); $\delta^{238}U$ supercomposite, ±1SD/(j) Andersen et al. (2015) and Noordmann et al. (2016) $\delta^{238}U$ data, ±1SE.

Altered oceanic crust										
Site	Age (Ma)	Region	~DIB (m)	Zone covered	Spreading type	U MORB (ng/g)	U AOC (ng/g)	U enrichment (ng/g)	$\delta^{238}U$ (‰)	±SE/SD
332/333*	3.5	Atlantic	600	Volcanic	Slow	100	253	153[a]		
504B	5.9	E. Pacific	2000	Volcanic	Intermediate	16	55	39[b]		
U1382/ 1383	8	Atlantic	600	Volcanic	Slow	60	140	80[c]		
1256	15	Pacific	1600	Volcanic/SD/ Gabbro	Fast	50	113	63[d]	−0.51[g]	0.15
417/418	120	Atlantic	550		Slow	35	321	286[e]	−0.20[h]	0.11
801	167	W. Pacific	400	Volcanic	Fast	44	390	346[f]	−0.17[i]	0.03
									−0.23[j]	0.08

the older Sites 801 (~167 Ma) and 417/418 (~120 Ma), with U excess estimates based on composite samples (Kelley et al., 2005; Kelley et al., 2003; Staudigel et al., 1996), show significantly higher U enrichments (346 ng/g and 286 ng/g, respectively) (Fig. 10).

It is also possible to estimate the mean $\delta^{238}U$ for the altered ocean crust sections at Sites 1256, 801, 417/418, where both U concentration and $\delta^{238}U$ data is available. The U concentrated-weighted mean of discrete samples from Site 1256 gives a $\delta^{238}U$ of −0.37 ± 0.07 ‰ (standard error of the mean). Taken the U concentrated mean using the length-scale of the lithology sections (excluding the plutonic dike-gabbro section) gives a lower $\delta^{238}U$ of −0.51 ± 0.15 ‰ (SD), which is likely a more representative value. This estimate is lower than the U concentrated-weighted mean $\delta^{238}U$ of the discrete samples at Site 417/

418 of −0.20 ± 0.11 ‰ and Site 801 of −0.23 ± 0.08 ‰ (standard error of the mean) (data; Andersen et al., 2015; Noordmann et al., 2016). The Site 801 U concentration-weighted mean $\delta^{238}U$ overlaps with the estimate of the supercomposite at Site 801 of −0.17 ± 0.03 ‰ (Fig. 10). The lower mean $\delta^{238}U$ for Site 1256 suggests relatively more oxidised U uptake compared to more reducing U uptake at the older Sites 801 and 417/418. A continuous low-temperature U uptake of more reducing character, beyond the ~15 million year age of Site 1256, could explain the higher U concentration and mean $\delta^{238}U$ estimates for the older Sites 417/418 and 801. Another possible scenario for the difference could be related to the lava pond at Site 1256, which may have restricted and minimized the seawater-derived circulation and thereby the U uptake during the more reductive U uptake phase compared to the older sites. A

Fig. 10. Crustal age versus estimated U addition (a) and $\delta^{238}U$ (b) for a range of altered oceanic crust sites. (a) the U addition is calculated from the measured sample U concentrations with estimated protolith subtracted (see Table 3 for details). (b) shows the weighted $\delta^{238}U$ mean composition for Sites 1256, 417/418 and 801. Site 801 also includes the measured supercomposite (artificially slightly separated in age to allow comparison to the weighted mean). See Table 3 for data sources and uncertainty estimates. The mean MORB $\delta^{238}U$ (Andersen et al. 2015) is shown for reference.

combination of the two processes is perhaps the likely explanation to the evolution of the U and its isotope systematics at Site 1256 compared to Sites 801 and 417/418.

6. Concluding remarks

The U concentration and isotope systematics at Site 1256 and other altered ocean crustal sites show that the overall U uptake and associated isotope compositions are both spatially and temporally heterogenous. The distribution of $\delta^{234}U$ disequilibrium through Site 1256 shows that U uptake from seawater-derived fluids appears active after 15 million years (albeit to a minor extent). This is surprising given little evidence for active seawater recharge into the ocean crust presently at Site 1256. This observation, however, is generally consistent with discernible regional conductive heat flow anomalies extending into ocean crust of ~65 Ma suggesting on-going hydrothermal transport of heat and low temperature ocean crust alteration (e.g., Parsons and Sclater, 1977; Stein and Stein, 1994). A change in the mean $\delta^{238}U$ for altered ocean crust with increasing age, i.e. between Site 1256 and sites on older crust (801, 417/418), is likely driven by the more reductive character of alteration and U uptake over time. This temporal evolution of seawater-derived fluid flow with a change from more oxidised to reduced conditions during low temperature alteration, may also play an important role for constraining the overall systematics of other redox-sensitive elements and their isotopes in altered ocean crust such as Tl and Mo (e.g. Coggon et al., 2014; Freymuth et al., 2015; Nielsen et al., 2006). Further work should focus on combining detailed studies of alteration assemblages with the U uptake and associated U isotope systematics, as well as community efforts for generating quantitatively representative new composite samples at different altered ocean crust sites. Better knowledge on the $\delta^{238}U$ and U concentration of specific alteration assemblages provide improved input values for models of the behaviour and release of U during prograde metamorphism during subduction and its deep cycling beyond the arc front. Furthermore, as shown from the $\delta^{234}U$ at Site 1256, U-series disequilibrium systematics may provide important constraints on the timescales of U mobility during low temperature alteration and convective heat fluxes in ageing altered ocean crust.

Data availability

Data are available at Mendeley Data at https://doi.org/10.17632/hgnkxhhh2x.1.

CRediT authorship contribution statement

Morten B. Andersen: Writing – review & editing, Writing – original draft, Project administration, Methodology, Investigation, Funding acquisition, Formal analysis, Conceptualization. **Joel B. Rodney:** Writing – review & editing, Investigation, Formal analysis. **Heye Freymuth:** Writing – review & editing. **Flurin Vils:** Writing – review & editing, Formal analysis. **Michelle Harris:** Writing – review & editing, Formal analysis. **Kari Cooper:** Writing – review & editing, Investigation. **Damon A.H. Teagle:** Writing – review & editing, Investigation. **Tim Elliott:** Writing – review & editing, Methodology, Investigation, Funding acquisition.

Declaration of competing interest

The authors declare that they have no known competing financial interests or personal relationships that could have appeared to influence the work reported in this paper.

Appendix A. Supplementary material

Geochemical data obtained during this study is available in supplementary tables. Supplementary material to this article can be found online at https://doi.org/10.1016/j.gca.2024.07.028.

References

Albarède, F., Michard, A., 1986. Transfer of continental Mg, S, O and U to the mantle through hydrothermal alteration of the oceanic crust. Chem. Geol. 57 (1–2), 1–15.

Alt, J.C., 1995. Sulfur isotopic profile through the oceanic crust: sulfur mobility and seawater-crustal sulfur exchange during hydrothermal alteration. Geology 23 (7), 585–588.

Alt, J.C., Laverne, C., Coggon, R.M., Teagle, D.A., Banerjee, N.R., Morgan, S., Smith-Duque, C.E., Harris, M., Galli, L., 2010. Subsurface structure of a submarine hydrothermal system in ocean crust formed at the East Pacific Rise, ODP/IODP Site 1256. Geochem. Geophys. Geosyst. 11 (10).

Alt, J.C., Teagle, D.A., 1999. The uptake of carbon during alteration of ocean crust. Geochim. Cosmochim. Acta 63 (10), 1527–1535.

Alt, J.C., Teagle, D.A., 2003. Hydrothermal alteration of upper oceanic crust formed at a fast-spreading ridge: mineral, chemical, and isotopic evidence from ODP Site 801. Chem. Geol. 201 (3), 191–211.

Andersen, M.B., Erel, Y., Bourdon, B., 2009. Experimental evidence for U-234-U-238 fractionation during granite weathering with implications for U-234/U-238 in natural waters. Geochim. Cosmochim. Acta 73 (14), 4124–4141.

Andersen, M.B., Vance, D., Keech, A.R., Rickli, J., Hudson, G., 2013. Estimating U fluxes in a high-latitude, boreal post-glacial setting using U-series isotopes in soils and rivers. Chem. Geol. 354, 22–32.

Andersen, M.B., Elliott, T., Freymuth, H., Sims, K.W., Niu, Y., Kelley, K.A., 2015. The terrestrial uranium isotope cycle. Nature 517 (7534), 356–359.

Andersen, M., Romaniello, S., Vance, D., Little, S., Herdman, R., Lyons, T., 2014. A modern framework for the interpretation of 238U/235U in studies of ancient ocean redox. Earth Planet. Sci. Lett. 400, 184–194.

Andersen, M.B., Stirling, C.H., Weyer, S., 2017. Uranium isotope fractionation. Rev. Mineral. Geochem. 82 (1), 799–850.

Bach, W., Peucker-Ehrenbrink, B., Hart, S.R., Blusztajn, J.S., 2003. Geochemistry of hydrothermally altered oceanic crust: DSDP/ODP Hole 504B – implications for seawater-crust exchange budgets and Sr- and Pb-isotopic evolution of the mantle. Geochem. Geophys. Geosyst. 4 (3), 8904.

Bacon, M.P., 1978. Radioactive disequilibrium in altered mid-oceanic basalts. Earth Planet. Sci. Lett. 39 (2), 250–254.

Basu, A., Brown, S.T., Christensen, J.N., DePaolo, D.J., Reimus, P.W., Heikoop, J.M., Woldegabriel, G., Simmons, A.M., House, B.M., Hartmann, M., 2015. Isotopic and geochemical tracers for U (VI) reduction and U mobility at an in situ recovery U mine. Environ. Sci. Technol. 49 (10), 5939–5947.

Bigeleisen, J., 1996. Nuclear size and shape effects in chemical reactions. Isotope chemistry of heavy elements. J. Am. Chem. Soc. 118, 3676–3680.

Bopp IV, C.J., Lundstrom, C.C., Johnson, T.M., Glessner, J.J., 2009. Variations in 238U/235U in uranium ore deposits: isotopic signatures of the U reduction process? Geology 37 (7), 611–614.

Brennecka, G.A., Wasylenki, L.E., Bargar, J.R., Weyer, S., Anbar, A.D., 2011. Uranium isotope fractionation during adsorption to Mn-oxyhydroxides. Environ. Sci. Technol. 45 (4), 1370–1375.

Chen, J., Wasserburg, G., Von Damm, K., Edmond, J., 1986. The U-Th-Pb systematics in hot springs on the East Pacific Rise at 21 N and Guaymas Basin. Geochim. Cosmochim. Acta 50 (11), 2467–2479.

Cheng, H., Edwards, R.L., Sehe, C.C., Polyak, V.J., Asmerom, Y., Woodhead, J., Hellstrom, J., Wang, Y., Kong, X., Spoetl, C., Wang, X., Alexander Jr, E.C., 2013. Improvements in 230Th dating, 230Th and 234U half-life values, and U-Th isotopic measurements by multi-collector inductively coupled plasma mass spectrometry. Earth Planet. Sci. Lett. 371–372, 82–91.

Coggon, R.M., Rehkämper, M., Atteck, C., Teagle, D.A., Alt, J.C., Cooper, M.J., 2014. Controls on thallium uptake during hydrothermal alteration of the upper ocean crust. Geochim. Cosmochim. Acta 144, 25–42.

Cuney, M., 2010. Evolution of uranium fractionation processes through time: driving the secular variation of uranium deposit types. Econ. Geol. 105 (3), 553–569.

Dunk, R.M., Mills, R.A., Jenkins, W.J., 2002. A reevaluation of the oceanic uranium budget for the Holocene. Chem. Geol. 190 (1–4), 45–67.

Elderfield, H., Schultz, A., 1996. Mid-ocean ridge hydrothermal fluxes and the chemical composition of the ocean. Annu. Rev. Earth Planet. Sci. 24, 191–224.

Fisher, A., Becker, K., Narasimhan, T., 1994. Off-axis hydrothermal circulation: parametric tests of a refined model of processes at Deep Sea Drilling Project/Ocean Drilling Program site 504. J. Geophys. Res. Solid Earth 99 (B2), 3097–3121.

Freymuth, H., Vils, F., Willbold, M., Taylor, R.N., Elliott, T., 2015. Molybdenum mobility and isotopic fractionation during subduction at the Mariana arc. Earth Planet. Sci. Lett. 432, 176–186.

Gale, A., Dalton, C.A., Langmuir, C.H., Su, Y., Schilling, J.G., 2013. The mean composition of ocean ridge basalts. Geochem. Geophys. Geosyst. 14 (3), 489–518.

Gao, Y., Vils, F., Cooper, K., Banerjee, N., Harris, M., Hoefs, J., Teagle, D., Casey, J., Elliott, T., Laverne, C., 2012. Downhole variation of lithium and oxygen isotopic compositions of oceanic crust at East Pacific Rise, ODP Site 1256. Geochem. Geophys. Geosyst. 13 (10).

Goto, K.T., Anbar, A.D., Gordon, G.W., Romaniello, S.J., Shimoda, G., Takaya, Y., Tokumaru, A., Nozaki, T., Suzuki, K., Machida, S., 2014. Uranium isotope systematics of ferromanganese crusts in the Pacific Ocean: implications for the marine 238U/235U isotope system. Geochim. Cosmochim. Acta 146, 43–58.

Harris, M., 2011. The Accretion of Lower Oceanic Crust. University of Southampton. Ph. D thesis.

Harris, M., Coggon, R.M., Smith-Duque, C.E., Cooper, M.J., Milton, J.A., Teagle, D.A., 2015. Channelling of hydrothermal fluids during the accretion and evolution of the upper oceanic crust: Sr isotope evidence from ODP Hole 1256D. Earth Planet. Sci. Lett. 416, 56–66.

Höfig, T.W., Geldmacher, J., Hoernle, K., Hauff, F., Duggen, S., Garbe-Schönberg, D., 2014. From the lavas to the gabbros: 1.25 km of geochemical characterization of upper oceanic crust at ODP/IODP Site 1256, eastern equatorial Pacific. Lithos 210, 289–312.

Huang, J., Ke, S., Gao, Y., Xiao, Y., Li, S., 2015. Magnesium isotopic compositions of altered oceanic basalts and gabbros from IODP site 1256 at the East Pacific Rise. Lithos 231, 53–61.

Israelson, C., Bjorck, S., Hawkesworth, C.J., Possnert, G., 1997. Direct U-Th dating of organic- and carbonate-rich lake sediments from southern Scandinavia. Earth Planet. Sci. Lett. 153 (3–4), 251–263.

Jemison, N.E., Johnson, T.M., Shiel, A.E., Lundstrom, C., 2016. Uranium isotope fractionation induced by U (VI) adsorption onto common aquifer minerals. Environ. Sci. Technol. 50 (22), 12232–12240.

Jenner, F.E., O'Neill, H.S.C., 2012. Analysis of 60 elements in 616 ocean floor basaltic glasses. Geochem. Geophys. Geosyst. 13 (2).

Kelley, K.A., Plank, T., Ludden, J., Staudigel, H., 2003. Composition of altered oceanic crust at ODP Sites 801 and 1149. Geochem. Geophys. Geosyst. 4 (6).

Kelley, K.A., Plank, T., Farr, L., Ludden, J., Staudigel, H., 2005. Subduction cycling of U, Th, and Pb. Earth Planet. Sci. Lett. 234 (3), 369–383.

Kigoshi, K., 1971. Alpha-recoil thorium-234 - dissolution into water and uranium-234/uranium-238 disequilibrium in nature. Science 173 (3991), 47.

Kipp, M.A., Li, H., Ellwood, M.J., John, S.G., Middag, R., Adkins, J.F., Tissot, F.L., 2022. 238U, 235U and 234U in seawater and deep-sea corals: a high-precision reappraisal. Geochim. Cosmochim. Acta 336, 231–248.

Kuhn, T., Versteegh, G., Villinger, H., Dohrmann, I., Heller, C., Koschinsky, A., Kaul, N., Ritter, S., Wegorzewski, A., Kasten, S., 2017. Widespread seawater circulation in 18–22 Ma oceanic crust: impact on heat flow and sediment geochemistry. Geology 45 (9), 799–802.

Li, H., Tissot, F.L., 2023. UID: the uranium isotope database. Chem. Geol. 618, 121221.

Macdougall, J., Finkel, R., Carlson, J., Krishnaswami, S., 1979. Isotopic evidence for uranium exchange during low-temperature alteration of oceanic basalt. Earth Planet. Sci. Lett. 42 (1), 27–34.

Michard, A., Albarede, F., Michard, G., Minster, J., Charlou, J., 1983. Rare-earth elements and uranium in high-temperature solutions from East Pacific Rise hydrothermal vent field (13 N). Nature 303 (5920), 795–797.

Mills, R.A., Dunk, R.M., 2010. Tracing low-temperature fluid flow on ridge flanks with sedimentary uranium distribution. Geochem. Geophys. Geosyst. 11 (8).

Mitchell, W.S., Aumento, F., 1977. Uranium in oceanic rocks: DSDP Leg 37. Can. J. Earth Sci. 14 (4), 794–808.

Mottl, M., Wheat, G., Baker, E., Becker, N., Davis, E., Feely, R., Grehan, A., Kadko, D., Lilley, M., Massoth, G., 1998. Warm springs discovered on 3.5 Ma oceanic crust, eastern flank of the Juan de Fuca Ridge. Geology 26 (1), 51–54.

Murphy, M.J., Stirling, C.H., Kaltenbach, A., Turner, S.P., Schaefer, B.F., 2014. Fractionation of 238U/235U by reduction during low temperature uranium mineralisation processes. Earth Planet. Sci. Lett. 388, 306–317.

Nielsen, S.G., Rehkämper, M., Teagle, D.A., Butterfield, D.A., Alt, J.C., Halliday, A.N., 2006. Hydrothermal fluid fluxes calculated from the isotopic mass balance of thallium in the ocean crust. Earth Planet. Sci. Lett. 251 (1–2), 120–133.

Nisbet, H., Migdisov, A.A., Williams-Jones, A.E., Xu, H., van Hinsberg, V.J., Roback, R., 2019. Challenging the thorium-immobility paradigm. Sci. Rep. 9 (1), 17035.

Noordmann, J., Weyer, S., Georg, R.B., Jöns, S., Sharma, M., 2016. 238U/235U isotope ratios of crustal material, rivers and products of hydrothermal alteration: new insights on the oceanic U isotope mass balance. Isot. Environ. Health Stud. 52 (1–2), 141–163.

Palmer, M.R., Edmond, J.M., 1989. The strontium isotope budget of the modern ocean. Earth Planet. Sci. Lett. 92 (1), 11–26.

Parsons, B., Sclater, J.G., 1977. An analysis of the variation of ocean floor bathymetry and heat flow with age. J. Geophys. Res. 82 (5), 803–827.

Patten, C.G., Pitcairn, I.K., Teagle, D.A., Harris, M., 2016. Sulphide mineral evolution and metal mobility during alteration of the oceanic crust: insights from ODP Hole 1256D. Geochim. Cosmochim. Acta 193, 132–159.

Pavia, F.J., Cooperdock, E.H., de Obeso, J.C., Sims, K.W., Tissot, F.L., Klein, F., 2023. Uranium isotopes as tracers of serpentinite weathering. Earth Planet. Sci. Lett. 623, 118434.

Plank, T., Ludden J., Escutia C., Abrams L., Alt J., Armstrong R., Barr S., Bartolini A., Cairns G., Fisk M., Guerin G., Haveman S., Hirono T., Honnorez J., Kelley K., Larson R., Lozar F., Murray R., Pletsch T., Pockalny R., Rouxel O., Schmidt A., Smith D., Spivack A., Staudigel H., Steiner M., Valentine R., 2000. Proceedings of the Ocean Drilling Program, Initial Reports. Ocean Drilling Program, College Station, TX, pp. 185.

Plank, T., Manning, C.E., 2019. Subducting carbon. Nature 574 (7778), 343–352.

Porcelli, D., Swarzenski, P.W., 2003. The behavior of U- and Th-series nuclides in groundwater. Uranium-Ser. Geochem. 317–361.

Reyss, J.L., Lemaitre, N., Bonté, P., Franck, D., 1987. Anomalous 234U/238U ratios in deep-sea hydrothermal deposits. Nature 325 (6107), 798–800.

Richter, S., Alonso-Munoz, A., Eykens, R., Jacobsson, U., Kuehn, H., Verbruggen, A., Aregbe, Y., Wellum, R., Keegan, E., 2008. The isotopic composition of natural uranium samples—measurements using the new *n*(233U)/*n*(236U) double spike IRMM-3636. Int. J. Mass Spectrom. 269 (1), 145–148.

Romaniello, S.J., Herrmann, A.D., Anbar, A.D., 2013. Uranium concentrations and 238U/235U isotope ratios in modern carbonates from the Bahamas: assessing a novel paleoredox proxy. Chem. Geol. 362, 305–316.

Staudigel, H., 2003. Hydrothermal alteration processes in the oceanic crust. Treatise Geochem. 3, 511–535.

Staudigel, H., 2014. Chemical fluxes from hydrothermal alteration of the oceanic crust. Treatise Geochem. 583–606.

Staudigel, H., Hart, S.R., Schmincke, H.-U., Smith, B.M., 1989. Cretaceous ocean crust at DSDP Sites 417 and 418: carbon uptake from weathering versus loss by magmatic outgassing. Geochim. Cosmochim. Acta 53 (11), 3091–3094.

Staudigel, H., Davies, G.R., Hart, S.R., Marchant, K.M., Smith, B.M., 1995. Large scale isotopic Sr, Nd and O isotopic anatomy of altered oceanic crust: DSDP/ODP sites417/418. Earth Planet. Sci. Lett. 130 (1), 169–185.

Staudigel, H., Plank, T., White, B., Schmincke, H.-U., 1996. Geochemical fluxes during seafloor alteration of the basaltic upper oceanic crust: DSDP Sites 417 and 418. Geophys. Monogr. Ser. 96, 19–38.

Stein, C.A., Stein, S., 1994. Constraints on hydrothermal heat flux through the oceanic lithosphere from global heat flow. J. Geophys. Res. Solid Earth 99 (B2), 3081–3095.

Stirling, C.H., Andersen, M.B., Potter, E.-K., Halliday, A.N., 2007. Low temperature Isotope Fractionation of uranium. Earth Planet. Sci. Lett. 264, 208–225.

Teagle, D., Alt, J., Halliday, A., 1998. Tracing the evolution of hydrothermal fluids in the upper oceanic crust: Sr-isotopic constraints from DSDP/ODP Holes 504B and 896A. Geol. Soc. Lond. Spec. Publ. 148 (1), 81–97.

Teagle, D., Alt, J., Umino, S., Miyashita, S., Banerjee, N., Wilson, D., Coggon, R., 2006. An intact section of ocean crust formed at a superfast spreading rate.

Teagle, D.A.H., Ildefonse, B., Blum, P., and the Expedition 335 Scientists, 2012. Expedition 335 summary. Proceedings of the Integrated Ocean Drilling Program 335.

Tissot, F.L., Dauphas, N., 2015. Uranium isotopic compositions of the crust and ocean: age corrections, U budget and global extent of modern anoxia. Geochim. Cosmochim. Acta 167, 113–143.

Tominaga, M., Teagle, D.A., Alt, J.C., Umino, S., 2009. Determination of the volcanostratigraphy of oceanic crust formed at superfast spreading ridge: electrofacies analyses of ODP/IODP Hole 1256D. Geochem. Geophys. Geosyst. 10 (1).

Türke, A., Nakamura, K., Bach, W., 2015. Palagonitization of basalt glass in the flanks of mid-ocean ridges: implications for the bioenergetics of oceanic intracrustal ecosystems. Astrobiology 15 (10), 793–803.

Vance, D., Teagle, D.A.H., Foster, G.L., 2009. Variable Quaternary chemical weathering fluxes and imbalances in marine geochemical budgets. Nature 458 (7237), 493–496.

Villinger, H., Pichler, T., Kaul, N., Stephan, S., Pälike, H., Stephan, F., 2017. Formation of hydrothermal pits and the role of seamounts in the Guatemala Basin (equatorial East Pacific) from heat flow, seismic, and core studies. Geochem. Geophys. Geosyst. 18 (1), 369–383.

Weyer, S., Anbar, A.D., Gerdes, A., Gordon, G.W., Algeo, T.J., Boyle, E.A., 2008. Natural fractionation of 238U/235U. Geochim. Cosmochim. Acta 72 (2), 345–359.

Wilson, D.S., Teagle, D.A.H., Alt, J.C., Banerjee, N.R., Umino, S., Miyashita, S., Acton, G. D., Anma, R., Barr, S.R., Belghoul, A., 2006. Drilling to gabbro in intact ocean crust. Science 312 (5776), 1016–1020.